Arithmetic variance swaps

Article (Accepted Version)

Arithmetic Variance Swaps

Stamatis Leontsinis[a] and Carol Alexander[b]

[a] RwC Asset Management, London

[b] School of Business, Management and Economics, University of Sussex

To appear in Quantitative Finance, 2016 (in press)

Abstract

Biases in standard variance swap rates can induce substantial deviations below market rates. Defining realised variance as the sum of squared price (not log-price) changes yields an 'arithmetic' variance swap with no such biases. Its fair value has advantages over the standard variance swap rate: no discrete-monitoring or jump biases; and the same value applies for any monitoring frequency, even irregular monitoring and to any underlying, including those taking zero or negative values. We derive the fair-value for the arithmetic variance swap and compare with the standard variance swap rate by: analysing errors introduced by interpolation and integration techniques; numerical experiments for approximation accuracy; and using 23 years of FTSE 100 options data to explore the empirical properties of arithmetic variance (and higher-moment) swaps. The FTSE 100 variance risk has a strong negative correlation with the implied third moment, which can be captured using a higher-moment arithmetic swap.

JEL Code: G01, G12, G15

Keywords: Fourth Moment Swap, Hermite Spline, Kurtosis, Model-Free, Realised Variance, Skewness, Third Moment Swap, Volatility Index, VIX, VFTSE.

1 Introduction

A standard variance swap on a traded asset initiated at time t and expiring at $T > t$ is a forward contract which pays a fixed strike $\bar{K}$, called the variance swap rate (VSR), and receives the realised variance $\mathrm{RV}_{t,T}$ from time t to time T. The buyer of notional N on a vanilla variance swap has pay-off $N\left[\mathrm{RV}_{t,T} - \bar{K}\right]$ and the fair-value of the VSR $\bar{K}$ at initiation, $K_{t,T}$, is the risk-neutral expectation of $\mathrm{RV}_{t,T}$. While the two parties may enter the swap at any market rate $\bar{K}$ which they can agree, each should enter the agreement having some idea of its fair value, $K_{t,T}$. A formula for this fair value is derived by assuming certain properties for the underlying price process and is implemented using integration over vanilla option prices. If they use different price process assumptions, and/or employ different numerical methods for implementation, the two parties will not exactly agree on the fair-value rate.

Since the mid 1990's variance swaps have been actively traded over the counter (OTC) for volatility speculation, equity diversification, dispersion trading and both vega and correlation hedging; see Clark [2010] for more details. Normally it pays to write variance swaps because the variance risk premium is typically small and negative, but during volatile periods it can be very large and positive, so potential losses on short variance swap positions can be large. Figure 1 depicts the pay-off to the long realised variance party in a 30-day S&P 500 variance swap, on the right-hand scale, in \$000 per \$1 notional. For instance, by October 2008 the realised legs had diverged substantially above the swap rates that were struck before the Lehman Brother's collapse. At this time, a bank that issued \$10m notional on an S&P variance swap would be obliged to pay out \$10bn to their counter-party.

Using market quotes instead of the synthesised rates employed in previous research, Konstantinidi and Skiadopoulos [2016] show that a dealer's funding liquidity has a substantial effect on the variance risk premium. Their trading-activity model predicts the market variance risk premium much better than a variety of alternative predictive models and the premium becomes significantly more negative when funding illiquidity increases, i.e. when

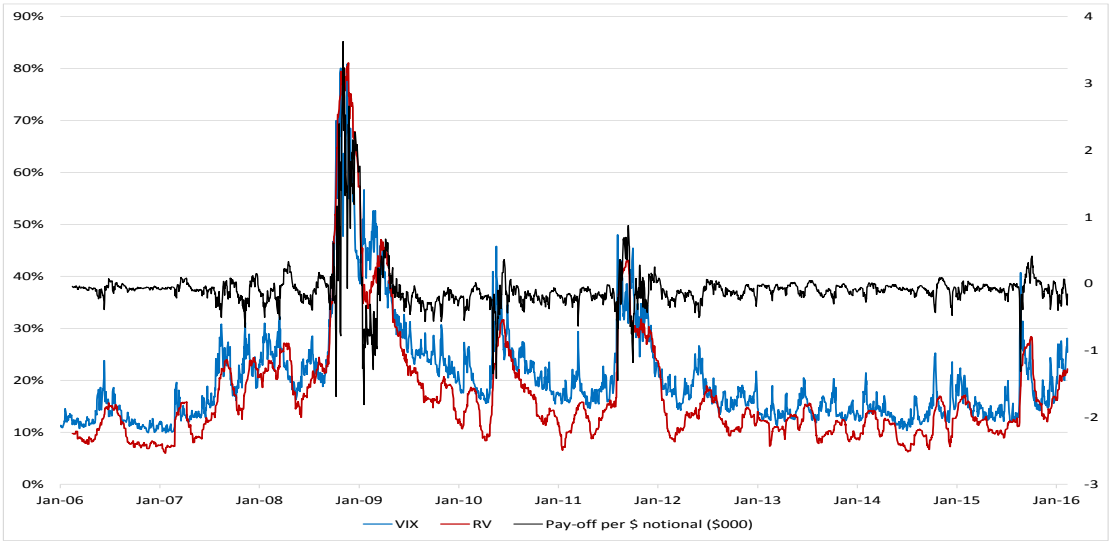

Figure 1: Pay-Off to S&P 500 Variance Swaps: Long Realised Variance
January 2006 – December 2015: The VIX index is shown in blue and realised variance in red, on the left-hand axis; The pay-off in $000 to $1 notional long realised variance is in black and measured on the right-hand scale.

trading conditions deteriorate. Indeed, in extreme circumstances dealers may even cease to quote prices.[1]

Despite this liquidity risk, variance swaps remain actively traded OTC today and some innovative products are emerging. For instance: in April 2006 JP Morgan introduced corridor variance swaps, which limit the downside risk to both counter-parties by paying realised variance only when it is within a pre-defined range; in March 2009 Societé General launched the American variance swap; and since the banking crisis it has become standard to cap realised variance at 2.5 times the swap rate. In addition to conditional swaps and swaps with other features that limit the issuer's risk, there has been growing interest in variance swaps on oil, gold and other commodities, currencies and bonds.

The realised variance is specified in the terms and conditions of the contract – see JP-Morgan [2006] for an example. Typically, it is an average of squared daily log returns on

[1]For instance, some of the biggest dealers stopped providing single stock variance swaps as it became impossible to hedge them during the banking crisis. At this time equity option prices was soaring as demand for the insurance offered by OTM puts became impossible to supply. Consequently the VIX index, which represents the fair value of a variance swap on the S&P 500, spiked at a level exceeding 80% in October 2008, its highest value on record.

the underlying over the life of the swap. At the time of writing the Chicago Board Options Exchange (CBOE) quotes more than 30 volatility indices based on this definition of realised variance as the basis for listing volatility futures.[2] The underlyings range from index and single stock futures to iShares, commodity futures and interest rate futures. Most other major derivatives exchanges quote volatility indices based on the same, now standard, definition of realised variance as the CBOE.

Motivated by growing demand for trading and investing in volatility, this paper proposes an alternative variance swap as a new OTC contract for dealers to consider. In an 'arithmetic' variance swap the floating leg is an average of squared changes in the underlying price itself, rather than changes in the log price. An arithmetic variance swap accesses essentially the same risk premium as a standard variance swap. To see this, Figure 2 depicts the correlation between the standard and the arithmetic variance risk premia for the FTSE 100 index from the beginning of 1997 to the end of 2015. The average correlation is 0.9799 over the entire 19-year period, and it ranges from a minimum of 0.8658 to a maximum of 0.9985.

The innovative work of Neuberger [2012] and Bondarenko [2014] provide a further motivation for our research. These authors introduce a class of swaps for which an 'aggregation property' holds, and consequently the same fair-value swap rate formula applies whether the realised variance is monitored daily, weekly or even irregularly.[3] Arithmetic variance swaps satisfy this aggregation property, but standard variance swaps do not. Thus, arithmetic swaps have a trading advantage over standard variance swaps because their theoretical values should be closer to market rates – they are not influenced by the jump and discretisation biases that are problematic for standard variance swaps. By the same token, they are applicable to a wider variety of products, such as those that are monitored in transaction time.[4]

[2]Further details on the evolution of the exchange-traded market for volatility products over the last few years are given in Alexander et al. [2015].

[3]Note that Alexander and Rauch [2016] prove that the aggregation properties of Neuberger [2012] and Bondarenko [2014] are equivalent when Neuberger's definition is restricted to a bivariate process $\{F, \ln F\}$ with F being a martingale.

[4]This would increase the homoscedasticity of realised variance and hence lower the risk of purchasing effective volatility diversification for equity investors.

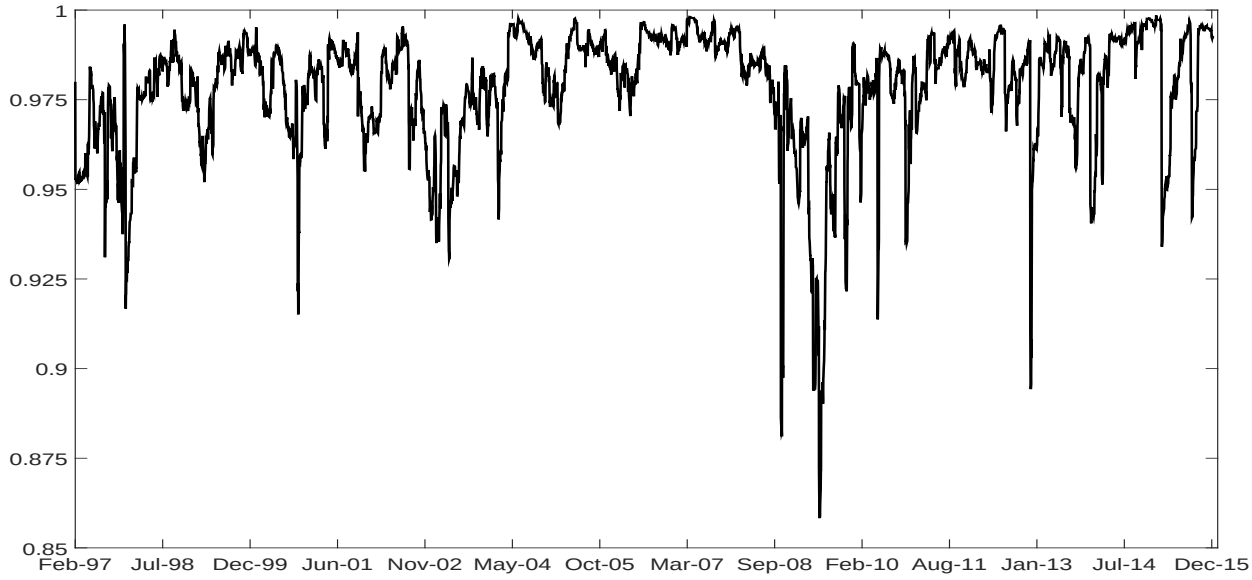

Figure 2: EWMA Correlation between AVRP and GVRP on FTSE 100
This graph shows the correlation between the daily percentage changes in the standard and the arithmetic variance risk premia for the FTSE 100 index, from January 1997 to December 2015. The correlation at each point in time is computed using an exponentially weighted moving average with smoothing constant 0.95.

Furthermore, the arithmetic definition allows these variance swaps to be traded on underlyings that could become negative, such as spreads, energy prices or (nowadays) interest rates. Obviously, a standard variance swap must be confined to an underlying that must always take a positive value.

Because the realised arithmetic variance satisfies the aggregation property, the only assumption required to derive an exact fair value for an arithmetic swap is that the underlying forward price follows a martingale, i.e. that the market for the underlying is free from arbitrage.[5] By contrast the fair value for the standard realised variance has jump errors and discrete-monitoring biases, both of which are large and negative during volatile periods, see Carr and Lee [2009] and Rompolis and Tzavalis [2013].[6] The combination of the two bi-

[5]The arithmetic variance swap is related to the 'simple' variance swap introduced by Martin [2013] where realised variance is an average sum of squared percentage price changes. However, the simple variance swap only applies to underlyings with positive prices, and it has the added disadvantage that it does not satisfy the aggregation property, so the discrete-monitoring error is not zero. However, in common with with our arithmetic variance swap, the replicating portfolio for a simple variance swap is equally weighted.

[6]However, Mueller et al. [2013], Du and Kapadia [2012] and others show that market variance swap rates can still be synthesised in the presence of jumps, provided a continuum of option strikes are traded, and that their pay-offs are proxied and/or that a specific trading strategy is followed.

ases can be very significant, in fact, market variance swap rates were sometimes more than 5% above the fair-value variance swap rate during the banking crisis, see Ait-Sahalia et al. [2014]. By contrast, because of its exact model-free fair value, there should be much less de-coupling of market quotes from fair values when arithmetic variance swaps are traded. Moreover the forward price does not need to be always positive, so arithmetic swaps have wider practical applications than standard variance swaps, including underlyings that may have zero or negative prices (e.g. a spread, a power price, or an interest rate).

The common fair-value formula for a standard variance swap is based on the first moment of the quadratic variation of the log return, and the replication portfolio weights option prices by the inverse of the square of the strike. Hence this portfolio places a relatively high weight on the low-strike put options which become highly illiquid during a market crisis.[7] By contrast, the arithmetic fair-value formula weights all options equally and, as such, its replication is less prone to distortion by stale prices of OTM put options.

We also derive fair-value formulae for higher-moment arithmetic swaps, showing that the replication portfolios for third- and fourth-moment arithmetic swaps are also equally-weighted OTM option portfolios. Compared with the higher moments of log returns, which can only be replicated by further increasing the weight on OTM put options (e.g. for the third-moment geometric swap the weight on an OTM option of strike K would be K^{-3}) higher-moment arithmetic swaps would certainly be less prone to liquidity risk.

The paper proceeds as follows: Section 2 describes the pricing of standard variance swaps and sets our work in the context of the recent literature; Section 3 derives the fair value for an arithmetic variance swap and the error when it is adapted to approximate the price of a standard variance swap; Section 4 discusses numerical interpolation and integration techniques; Section 5 presents a numerical study to compare the size of the errors when

[7] Another formula, introduced by Bakshi et al. [2003] and which also weights option prices by the inverse of the square of the strike, computes the fair value swap rate as the second moment of the log return distribution. Empirical results comparing these two swap rates are not presented in Section 6, for brevity, because when similar numerical interpolation and integration techniques are applied the two formulae yield almost identical results

we adjust each fair-value formula to approximate the other variance swap rate; Section 6 analyses the empirical characteristics of arithmetic variance and higher-moment swap rates with synthetic constant maturities from 30 to 270 days, using 23 years of historical data on FTSE 100 futures and options and market rate data from BNP-Paribas; Section 7 concludes. Detailed derivations, including fair-value expressions for arithmetic higher-moment swaps, are given in the Appendix.

2 Fair Values for Standard Variance Swaps

Assume a geometric diffusion process for the underlying price S_t:

$$\frac{dS_t}{S_t} = rdt + \sigma_t \, dB_t, \tag{1}$$

where r is the risk-free rate, assumed constant, and B_t is a Brownian motion. Writing the continuously-monitored realised variance from time t to time T as

$$\mathrm{RV}_{t,T} = (T-t)^{-1}\Sigma_{t,T}, \qquad \text{where} \qquad \Sigma_{t,T} = \int_{u=t}^{T} \sigma_u^2 \, du, \tag{2}$$

and denoting the expectation at time t under the risk-neutral measure by $\mathbb{E}_t[\cdot]$, the fair-value VSR is defined as

$$K_{t,T} = (T-t)^{-1}\mathbb{E}_t\left[\Sigma_{t,T}\right]. \tag{3}$$

Under the risk-neutral measure the fundamental theorem of asset pricing states that the value of a fixed-payer variance swap at inception time t should equal to 0, i.e. $\mathbb{E}_t\left[\Sigma_{t,T} - K_{t,T}\right] = 0$.

Neuberger [1994] shows that $\Sigma_{t,T}$ is the expected pay-off to a short position on a log contract, i.e. the contract with pay-off $\log\left(S_{_T}/S_t\right)$ at time T. The market is complete, under assumption (1), so the log contract pay-off and therefore also the realised variance can be replicated using vanilla options. In fact, there are two representations of $K_{t,T}$ in terms of call and put prices which are commonly employed. We label these $K_{t,T}$, $\tilde{K}_{t,T}$. To state these formulae in a form that is used by practitioners we use the following notation:

$F_{t,T} = e^{r(T-t)}S_t$ is the T-maturity forward price, and $\mathcal{Q}_t(k,T)$ is a fair-value vanilla put or call price of strike k and maturity T. Specifically, for $k < S^*_{t,T}$ it is the price of a vanilla put maturing at time T and for $k > S^*_{t,T}$ it is the corresponding call price. We use the same notation throughout for the separation strike $S^*_{t,T}$, i.e. the boundary separating the out-of-the-money call and put options. Typically this is the highest strike at or below $F_{t,T}$.

Demeterfi et al. [1999] derived the following time t option replication portfolio for the fair-value of a standard variance swap of maturity T:

$$K_{t,T} \;=\; 2(T-t)^{-1}\left\{e^{r(T-t)}\int_0^\infty \frac{\mathcal{Q}_t(k,T)}{k^2}\,dk - \frac{F_{t,T}-S^*_{t,T}}{S^*_{t,T}} - \ln\left(\frac{S^*_{t,T}}{S_t}\right)\right\}. \qquad (4)$$

An alternative variance swap rate formula computes the second moment of the log return rather than the first moment of the quadratic variation of the log return. With this approach, first used by Bakshi et al. [2003], there is no need to assume a specific dynamic process for the underlying asset price except that it is a positive semi-martingale. Applying the replication theorem of Carr and Madan [2002] to a contract with pay-off $\ln\left(S_{_T}/S_t\right)^2$ yields a formula which shares many similarities with (4), as discussed in the appendix.

The geometric diffusion assumption (1) of Demeterfi et al. [1999] can be generalised: Carr and Lee [2003] and Jiang and Tian [2005] show that (4) still holds under any type of diffusion for the stochastic volatility process σ_t including a coupled process with non-zero price-volatility correlation. Friz and Gatheral [2005] used Carr and Lee's results to derive an expression for the expectation of the square root of the quadratic variation of the returns, which is useful for pricing volatility derivatives. Gatheral [2006] also arrives at (4) using a model-free decomposition of the pay-off to a power option, by computing the first moment of the quadratic variation of the returns process assuming zero price-volatility correlation.

Broadie and Jain [2008] quantify the jump bias in (4) under various stochastic volatility models. Rompolis and Tzavalis [2013] derive bounds for the jump bias and demonstrate, via simulations and an empirical study, that price jumps induce a systematic negative bias that is particularly apparent during excessively volatile periods, when (4) significantly underesti-

mates the fair-value swap rate.

This negative jump bias is compounded by another theoretical bias which arises because the standard contract specifies realised variance as a discretely monitored average of squared log returns. In practice the realised variance is not continuously monitored and typically:

$$\mathrm{RV}_{t,T} = T_d^{-1}\Sigma_{t,T}^d = T_d^{-1}\sum_{i=t}^{T-1}\left(\log S_{i+1} - \log S_i\right)^2, \tag{5}$$

where T_d is the number of trading days between t and T. As shown by Carr and Lee [2009] the discrete-monitoring bias in (4) is typically negative and, like the jump bias, is most pronounced during volatile periods.[8] They prove that the discrete-monitoring error $\mathbb{E}_t[\Sigma_{t,T}] - \mathbb{E}_t[\Sigma_{t,T}^d]$ is proportional to $\sum_{i=t}^{T-1}\left[\frac{S_{i+1}-S_i}{S_i}\right]^3$ so it tends to be negative, and is especially large during volatile periods when (4) tends to underestimate fair-value swap rates considerably, due to jump and discrete-monitoring biases.

3 An Arithmetic Variance Swap Fair-Value Formula

Here, instead of the realised variance definition (5) we define the realised variance as

$$\mathrm{RV}_{t,T}^{*} = T_d^{-1}\sum_{i=t}^{T-1}\left(S_{i+1} - S_i\right)^2. \tag{6}$$

As explained in the introduction this approach has several advantages over the standard realised variance definition (5). The characteristic (6) does not suffer from discrete monitoring bias,[9] nor jump bias because satisfies the aggregation property of Neuberger [2012]. Hence it requires minimal, truly model-free assumptions. The only requirement is that the market is arbitrage-free, so that forward prices follow a martingale (which could be zero or negative). Moreover, being based on a distribution for the price level rather than the log return, it is

[8] There has been considerable recent research on this discrete-monitoring bias. For instance, Jarrow et al. [2013] derive discrete-monitoring error bounds that get tighter as the monitoring frequency increases and Bernard et al. [2014] generalise these results and provide conditions for signing the discrete-monitoring bias.

[9] Indeed monitoring could even be irregular, such as in trading time rather than calendar time.

more broadly applicable. One can always consider a density for S_T but it only makes sense to consider the density of $\log(S_T/S_t)$ when S_t is always positive. Otherwise the log return return does not exist so one cannot price a swap on standard realised variance.

In the following we present only the main result on the fair-value of an arithmetic variance swap under the risk-neutral measure for S_T as seen from time t. Full details of the derivations, including those for arithmetic higher-moment swaps, are given in the Appendix. Using the well-known result of Breeden and Litzenberger [1978], the risk-neutral moment generating function for S_T, denoted $\mathcal{M}_{t,T}(\lambda) = \mathbb{E}_t[\exp(\lambda S_T)]$ may be expressed as

$$\mathcal{M}_{t,T}(\lambda) = \int_{k=0}^{\infty} e^{\lambda k} \frac{\partial^2 \tilde{C}(k,T)}{\partial k^2}\, dk,$$

where for brevity we write $\tilde{C}(K,T) = e^{r(T-t)}C(k,T)$ and similarly for $\tilde{P}(k,T)$. Integrating by parts twice and using the following properties of call option prices:

$$\lim_{k\to 0}\tilde{C}(k) = S_T, \lim_{k\to+\infty}\tilde{C}(k) = 0, \lim_{k\to 0}\frac{\partial\tilde{C}(k)}{\partial k} = -1 \text{ and } \lim_{k\to+\infty}\frac{\partial\tilde{C}(k)}{\partial k} = 0,$$

we obtain :

$$\mathcal{M}_{t,T}(\lambda) = 1 + \lambda F_{t,T} + \lambda^2 \int_{k=0}^{\infty} e^{\lambda k}\tilde{C}(k,T)\, dk. \tag{7}$$

The n^{th} moment of the distribution of S_T is obtained by taking the n^{th} derivative of (7) with respect to λ and setting $\lambda = 0$. Thus, for $n = 1, 2, \ldots$

$$\mathbb{E}_t\left[S_T^n\right] = 1_{\{n=1\}}F_{t,T} + n(n-1)\int_{k=0}^{\infty} k^{n-2}\tilde{C}(k,T)\, dk. \tag{8}$$

Using the put-call parity relationship $\tilde{C}(k,T) - \tilde{P}(k,T) = F_{t,T} - k$ we transform (8) to include only OTM put and call options, with separation strike $S^*_{t,T}$. After some straightforward

calculations we have:

$$\mathbb{E}_t\left[S_T^2\right] = 2\left(F_{t,T} - S_{t,T}^*\right)S_{t,T}^* + \left(S_{t,T}^*\right)^2 + 2e^{r(T-t)}\int_{k=0}^{\infty}\mathcal{Q}_t\left(k,T\right)dk.$$

Since $\mathbb{E}_t\left[S_T\right] = F_{t,T}$, the second central moment of the risk-neutral density for S_T is:

$$\mathrm{V}_t\left[S_T\right] = 2e^{r(T-t)}\int_{k=0}^{\infty}\mathcal{Q}_t\left(k,T\right)dk - \left(F_{t,T} - S_{t,T}^*\right)^2. \tag{9}$$

The formula (9), when divided by $(T-t)$, is the fair value of a continuously-monitored arithmetic variance swap, applicable when the terms and conditions of the variance swap define realised variance as (6). Compared with the integral in (4) for the fair-value of the variance of log returns, (9) does not require that we weight option prices by the inverse of the square of the strike. With equal weighting of options in the replicating portfolio (9) issuers are less exposed to liquidity shortages in low strike put options during market crises.

Now we consider the special case that the underlying follows the geometric diffusion (1) with deterministic volatility in order to approximate the percentage return with the log return and thereby translate (9) into an approximate formula for the fair-value of variance of the log return. From $S_T = S_t\exp\left(r(T-t) - \frac{1}{2}\Sigma_{t,T} + \int_t^T \sigma_s dB_s\right)$, we have

$$\begin{aligned}
\mathbb{E}_t\left[S_T^2\right] &= S_t^2\exp\left(2r(T-t) - \Sigma_{t,T}\right)\mathbb{E}_t\left[\exp\left(2\int_t^T \sigma_s\, dB_s\right)\right] \\
&= S_t^2\exp\left(2r(T-t) - \Sigma_{t,T}\right)\exp\left(2\int_t^T \sigma_s^2\, ds\right), \\
&= S_t^2\exp\left(2r(T-t) + \Sigma_{t,T}\right) = F_{t,T}^2\exp\left(\Sigma_{t,T}\right).
\end{aligned}$$

Thus $\mathrm{V}_t\left[S_T\right] = \mathbb{E}_t\left[S_T^2\right] - F_{t,T}^2 = F_{t,T}^2\left[\exp\left(\Sigma_{t,T}\right) - 1\right]$, and so $\mathrm{V}_t\left[\ln\left(S_T/S_t\right)\right] \approx \mathrm{V}_t\left[\left(S_T/S_t\right) - 1\right] =$

$S_t^{-2}\mathrm{V}_t\left[S_{_T}\right] = \exp\left(2r(T-t)\right)\left[\exp\left(\Sigma_{t,T}\right)-1\right]$. So dividing (9) by $F_{t,T}^2$, we set

$$K_{t,T}^{*} = (T-t)^{-1}\left(2\,S_t^{-2}e^{r(T-t)}\int_{k=0}^{\infty}\mathcal{Q}_t\left(k,T\right)dk - \left(\frac{F_{t,T}-S_{t,T}^{*}}{F_{t,T}}\right)^2\right). \tag{10}$$

$K_{t,T}^{*}$ is an approximate VSR for a standard variance swap that is based on a fair-value expression for $\exp\left[\Sigma_{t,T}\right]-1$, rather than a risk-neutral expectation of $\Sigma_{t,T}$ itself. They are only the same to first order approximation. Indeed, $K_{t,T}^{*}$ has a systematic upward bias which increases with $\Sigma_{t,T}$.[10] There is no discrete-monitoring bias in the fair-value arithmetic swap rate (9), but when adapted to an approximation $K_{t,T}^{*}$ to the fair value for a standard variance swap the negative discrete-monitoring bias in GVSR is likely to affect its approximation.

In the following, when represented as annualised percentage volatilities: the standard variance swap rate $K_{t,T}$ is labelled $\mathrm{GVSR}_{t,T}$; we call $\mathrm{V}_t\left[S_{_T}\right]$ the arithmetic variance swap rate (AVSR); its approximation $K_{t,T}^{*}$ to the standard variance swap rate, is termed AVSR*; and, finally, we adapt the GVSR to approximate the fair-value for an arithmetic variance swap on multiplying $\mathrm{GVSR}_{t,T}$ by the forward price $F_{t,T}$.

4 Integration and Interpolation Techniques

In this section we describe the numerical techniques used for our empirical studies later in the paper. In the first sub-section we discuss the alternative maturity interpolation and extrapolation methods for computing synthetic, constant-maturity option prices. The second sub-section takes these prices and computes the integrals in (4) and (9), but each requires an infinite number of OTM put and call options on a continuum of strikes. We only have prices for the n discrete strikes of traded options available, so we discuss the biases that are introduced when different numerical integration procedures are employed.

[10] Since $\exp\left(\Sigma\right)-1>\Sigma$.

4.1 Maturity-Interpolation Error

Vanilla options have fixed maturity dates so interpolation between (and possibly extrapolation to) different maturities is required to compute synthetic rates with fixed terms. This is frequently performed by interpolating/extrapolating implied variances, rather than the volatilities, or the option prices themselves. Linear interpolation over variance (but not over volatility) precludes calender arbitrage. Also, the time-series properties of implied volatilities are considered to be smoother than those of market option prices.[11]

Exchanges use a variant of the implied variance interpolation/extrapolation approach, computing VSRs using the following procedure: (a) OTM put and call options are allocated to maturity baskets according to their time to expiration; (b) VSR sub-indices for each available expiration date are calculated, using formula (11); (c) the desired maturities for the term structure of VSRs are obtained by linearly interpolating and extrapolating the variance term structure implied by these indices;[12] (d) the square root of the interpolated variance is used to quote the index in percentage points.

The linear interpolation across implied variances in step (c) ensures no calendar arbitrage, but empirically, implied variance does not grow linearly with term except at long maturities. So instead each segment is interpolated using a cubic Hermite polynomial of the form $-e^{x^2/2}\frac{d^3}{dx^3}e^{-x^2/2}$. For more information on Hermite cubic spline and other spline interpolation techniques, see Fritsch and Carlson [1980] or De Boor [2001]. We choose Hermite splines because their 'shape preserving' feature prevents the interpolant from shooting up or down in response to small pricing errors in vanilla options. As such, they are more suitable than cubic splines for extrapolation.

To illustrate this Figure 3 compares standard, cubic and Hermite cubic spline fits to FTSE 100 implied variances, depicting their implied volatilities. Clearly, cubic splines are

[11] For instance, see Panigirtzoglou and Skiadopoulos [2004], Bliss and Panigirtzoglou [2004], Kostakis et al. [2011] and Neumann and Skiadopoulos [2012].

[12] CBOE has recently included SPX weekly options in the calculation of VIX. This means that there is extrapolation in maturity required in the calculation of VIX any more. However, this is not possible for other volatility indices as weekly options are not available for the corresponding equity indices.

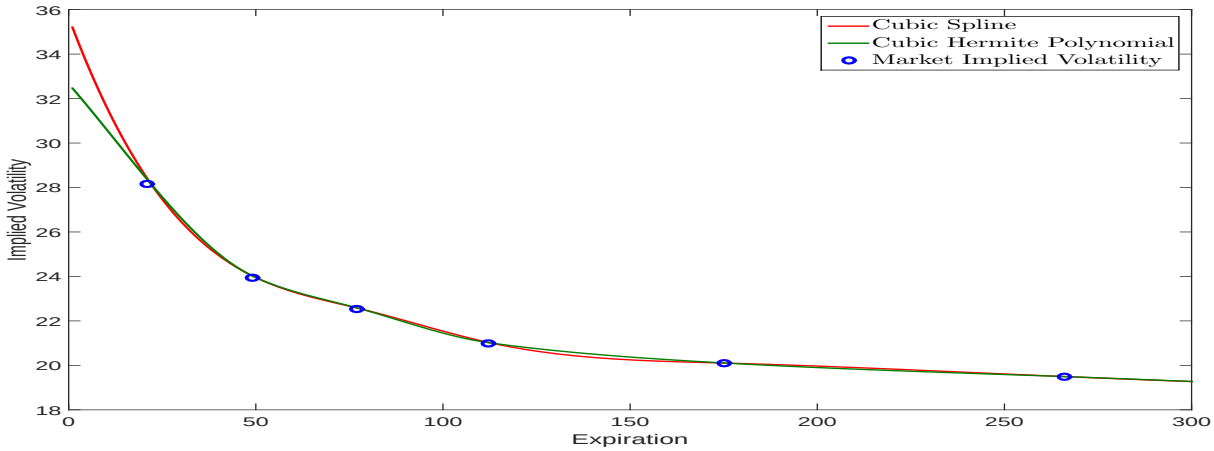

Figure 3: Spline vs Hermite Fitted Implied Volatility Term Structures
Illustration of cubic and Hermite cubic spline fits to FTSE 100 implied variances, reported as annual volatilities, on 30 March 2007.

too flexible; moreover, the choice of spline matters, as quite different volatility term structure shapes can result especially at the extreme long and short ends of the term structure. Hermite cubic spline interpolation and extrapolation results must, of course, be checked for no calendar arbitrage.[13]

4.2 Strike-Discretisation Errors

The CBOE and other exchanges typically employ the following Riemann sum approximation to formula (4) as the basis for quoting volatility indices :

$$K_{t,T} \cong (T-t)^{-1}\left[2\sum_{i=1}^{n} k_i^{-2} e^{r(T-t)} \mathcal{Q}_i\left(k_i, T\right) \Delta k_i - \left(\frac{F_{t,T}}{k_0} - 1\right)^2\right] \tag{11}$$

where $\mathcal{Q}\left(k_i, T\right)$ is the price of the i^{th} OTM option with strike k_i and maturity T, and k_0 is the first strike available at or below $F_{t,T}$. Here $\Delta k = (k_{i+1} - k_{i-1})/2$ for strikes straddling the i^{th} OTM option, $\Delta k = k_2 - k_1$ for the lowest strike and $\Delta k = k_n - k_{n-1}$ for the highest strike. The downward bias which results from taking a limited strike range, the so-called 'truncation error' is well understood already – see Jiang and Tian [2005]. It can be considerable, especially in volatile market conditions.

[13] In our empirical study we use 23 years of daily data of vanilla options of maturities up to one year, and we found that this condition was violated less than 0.2% of the time.

Another numerical integration error, the 'strike-descretisation error', stems from having only a discrete set of strikes available within this range. This may be positive or negative, depending on the shape of the distribution of current option prices: the integral will be downward (upward) biased when the function is monotonically increasing (decreasing). Hence, it is under-estimated on the OTM put section (low strike options) over-estimated on the OTM call section (high strike options). An upward bias arises when the option price function is negatively skewed, which is typically the case. For instance, Figure 4 depicts the distribution of FTSE 100 30-day vanilla option prices by strike on 30 March 2007.

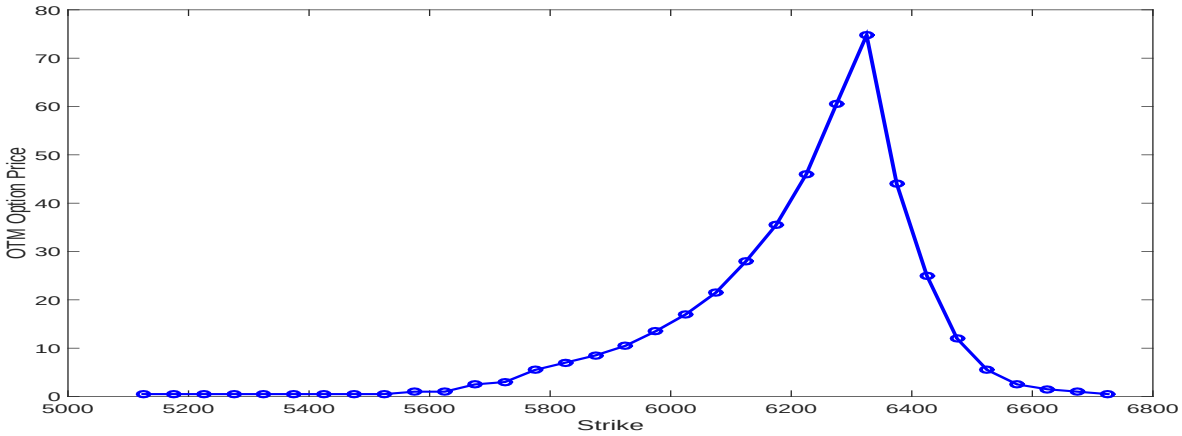

Figure 4: OTM Option Prices as a Function of Strike
30-day vanilla option prices derived via Hermite spline interpolation on implied variances between the April 2007 and May 2007 expiry dates on 30 March 2007.

Jiang and Tian [2007] favour alternative integration techniques such as cubic splines. The computation time is much slower than the Riemann sum, but in exceptionally volatile market conditions the use of cubic splines increases accuracy considerably relative to the Riemann sum. We now show that cubic spline integration also allows an analytic solution for the coefficients when the integral is over equally-weighted option prices. As such we can apply this formula to implement fair values for arithmetic moment swaps but numerical solution for the spline coefficients is still required to implement the fair value for a standard variance swap.

Fixing T and dropping the subscript for dependence on T, for brevity, the option price $\mathcal{Q}(k)$ is approximated with a cubic polynomial over the interval $[k_i, k_{i+1}]$ in the spline. If

there are n available strikes on date t for maturity T, each option price may be used as a knot point in the spline, so $\mathcal{Q}(k)$ is divided into $n-1$ third order polynomials of the form:

$$q_i(k) = a_i + b_i(k - k_i) + c_i(k - k_i)^2 + d_i(k - k_i)^3,$$

for $i = 1 \dots n-1$, and then

$$\int_{k=k_1}^{k_n} \mathcal{Q}(k)\, dk = \sum_{i=1}^{n-1} \int_{k=k_i}^{k_{i+1}} q_i(k)\, dk. \tag{12}$$

When the option prices are equally weighted in the swap rate, as they are for the arithmetic variance swap, there is a simple analytic formula for the integral based on cubic splines. This is because the standard spline continuity conditions for $\mathcal{Q}(k)$ are a system of $n-2$ recurrence equations in $n-2$ unknowns, which are easily solved for the coefficients a_i, b_i, c_i and d_i. Then some straightforward but tedious calculations yield the following for the total integral on the left:

$$\sum_{i=1}^{n-1} \frac{1}{12}(k_{i+1} - k_i)\left\{12a_i + (k_{i+1} - k_i)\left[6b_i + (k_{i+1} - k_i)\left(4c_i + 3d_i(k_{i+1} - k_i)\right)\right]\right\}. \tag{13}$$

Now numerical integration is unnecessary because each integral on the right of (12) can be solved analytically. Given the liquidity of FTSE 100 options and the plethora of strikes available we are able to evaluate integrals of option prices almost exactly by applying (13) to the available strikes at each maturity T.[14]

Table 1 compares the result of the equally-weighted option price integration based on the lower Riemann sum (as used by exchanges) with the analytic solution (13) for cubic splines. The first two columns distinguish between the calls and puts, where the Riemann sum has an upward and downward bias, respectively. We consider FTSE 100 options on 30 March

[14]Once the spline is fitted the computation time is extremely fast, being a simple analytic computation. For instance, on an Interl Core i7-3770 @ 3.4 GHz processor, with 16GB of memory 1 million integrations takes 1.08 microseconds, versus 7.27 microseconds for the Riemann sum.

2007 and 16 October 2008, these dates were chosen to represent relatively calm and volatile periods respectively (the FTSE 100 dropped by 5.5% on 16 October 2008). In both cases the lower Riemann sum overestimates the integral for OTM calls and underestimates the integral over OTM puts because of the negative skew in the price distribution. On 30 March 2007 the net upward bias on the Riemann sum is approximately 0.27%, but on 16 October 2008 (near the height of the banking crisis) the upward bias is greater, at $4046/409216 = 0.9\%$.

	OTM puts	**OTM calls**	**Total**
30 Mar 2007			
Lower Riemann Sum	13,825.0	8,337.5	22,162.5
Cubic Spline	15,681.3	6,420.8	22,102.1
16 Oct 2008			
Lower Riemann Sum	224,112.5	189,150.0	413,262.5
Cubic Spline	247,295.4	161,920.8	409,216.2

Table 1: Integral Approximation
Here we evaluate the equally-weighted option price integral using the lower Riemann sum and our analytic integration based on fitting the function using piecewise cubic splines. The Reimann sum has a net upward bias, due to the negative skewness in the option price function. The dates of the calculations are the 30^{th} March 2007 and the 16^{th} October 2008, randomly chosen as representative dates for low and high volatility.

5 Numerical Results

This section reports a numerical analysis on the relative accuracy of the GVSR and AVSR, comparing the truncation and strike-discretisation integration errors when each rate is used as an approximation to the other. The errors are measured relative to a 'true' VSR which is computed by assuming the option prices are determined by a price process. We suppose these are generated using two different geometric diffusions, a constant volatility geometric Brownian motion (GBM) and a stochastic volatility model with prices following the dynamics

in Heston [1993], viz.

$$\begin{aligned} dS_t &= (r)\, S_t dt + \sqrt{V_t} S_t dW_{1t}, \\ dV_t &= \kappa\,(\theta - V_t)\, dt + \eta\sqrt{V_t} dW_{2t}, \\ \langle dW_1, dW_2 \rangle &= \rho dt. \end{aligned}$$

These models yield closed-form option prices and thus allow a quick and easy computation of the fair-value swap rates without the need for simulation. We then compute the estimation error as the relative difference between the fair-value swap rate and the expected variance under the assumed price process.[15] Under GBM the expected variance is given by the constant volatility assumed in the model. With the Heston model, following Shreve [2004], the expected variance is:

$$T^{-1}\mathbb{E}\left[\sigma^2_{t,T}\right] = \frac{1-\exp(-\kappa T)}{\kappa T}\,(V_0 - \theta) + \theta.$$

In order to generate a skew in the option price distribution we assume the current underlying price S_0 is 80, 100 or 120, but keep fixed the option strike range and inter-strike interval. We set the interest rate to zero and select a volatility of either 20% or 50%. In the Heston model we set instantaneous volatility v_0 at 20% or 50%, the price-volatility correlation is fixed at -0.6, the long term variance θ is either 0.01 or 0.0625, the volatility of volatility η is 100% and the mean-reversion speed κ is either 1 or 5. These ranges are consistent with previous empirical studies on FTSE 100 dynamics, such as Kaeck and Alexander [2013]. For brevity, here we only present results for these parameters at the maturities 30 and 180 days but further results are available on request.

Table 2 reports the relative errors for the AVSR and its approximation derived from the standard VSR formula under GBM. By using an extreme strike range and a very fine strike grid we isolate the GVSR* errors in columns 5 – 8, demonstrating that they increase with

[15] Both expressed, as is conventional, as an annual volatility. For instance a 'true' model swap rate of 20% and a fair-value rate of 21% the relative error is 5%.

both maturity and volatility, as expected, but are unaffected by the skew in the distribution that is captured by setting the initial price at different levels. Columns 5 and 6 report the errors relative to the true volatility shown in column 2. These are large and negative for the GVSR*, indicating a substantial downward bias when the standard variance swap rate is used to approximate the AVSR.

Columns 9 – 12 report the truncation error by restricting the strike range in a manner that reflects the strikes typically available in financial markets, and here our discussion focusses on columns 11 and 12 for the AVSR. The truncation error induces a downward bias in the fair-value hence all errors are negative. They increase with maturity, as expected, as the distributions have a great range. It can be very high for very unlikely scenarios. For instance, the last row records an error of more than 10% for the AVSR, but this is at the six-month maturity and with a high and skewed implied volatility surface.

The last four columns report the strike discretisation errors. These are considerably higher for the GVSR* but this may be due to the superior numerical techniques that we employ for the AVSR. The main conclusion to draw from this table is that the estimation error that arises when the standard variance swap rate is adapted for pricing arithmetic variance swaps is considerable.

Table 3 reports the relative errors for the GVSR and its approximation AVSR* derived from the arithmetic VSR formula, this time under the dynamics (14) for the Heston stochastic volatility model. The Heston model parameters are set as described above and the GVSR in columns 4 and 5 are computed using (5). Again using an extreme strike range and a very fine strike grid to isolate the AVSR* errors in columns 7 and 8, we find that they are significantly negative. By contrast, the errors are minuscule for the GVSR. The truncation errors in the AVSR* shown in columns 9 and 10, and the strike discretisation errors in columns 13 and 14 are minimal compared with the initial approximation error. The stochastic volatility model also produces much larger errors for both swaps rates at the 180-day maturity, compared with Table 2, especially in the presence of a skew.

The main conclusion to draw from this section is that the two rates AVSR and GVSR suffer from similar numerical integration and truncation errors, each having a negative truncation bias which increases as the range of strikes narrows, and a positive skew integration bias that increases with the inter-strike range. Most importantly, the estimation errors that arise when one swap rate is used to approximate the other are very substantial.

6 Empirical Study

This section compares the empirical characteristics of the term structures of our two alternative fair-value formulae for a standard variance swap, i.e. (4) for the GVSR, implemented using the standard representation (11) of the swap rate, and (10) for the approximation adapted from the ASVR. Then we compare the 30-day swap rates with market variance swaps rates, focussing on the six-month period covering the banking crisis. Finally we depict the evolution of the term-structure of arithmetic skewness and kurtosis swap rates, discussing their empirical characteristics.

Daily closing prices for all vanilla European options traded on the FTSE 100 index from 2 October 1992 until 22 December 2015 were obtained from Optionmetrics (2002 – 2015) and Euronext (1992 – 2001). They contain in excess of 6 million data points. Although there are roughly equal numbers of in-the-money (ITM) and out-of-the-money (OTM) option prices, the trading volume on OTM options was approximately seven times greater than the volume traded in ITM options and we use only OTM calls and puts for the analysis. Then we apply standard filtering methods to remove particularly illiquid and thus stale option prices, and those with the minimum price. Finally, we apply the numerical procedures explained above, i.e. the GVSR is evaluated using the Riemann sum (11) and the AVSR is evaluated using the formula (13) for cubic spline integration.[16] The realised characteristics for the two swap rates are highly correlated, with their daily changes have a correlation of approximately 0.975 over the entire sample, which varies only slightly for different maturities.

[16]We omit results for the VSR (22) because they are very close to those for (11). They are available from the authors on request.

6.1 Features of the VFTSE Term Structure

Figure 5 depicts the VFTSE curve, represented by the GVSR, at maturities $30, 60, \ldots, 270$ calendar days between 2 October 1992 and 22 December 2015.[17] Both the Asian property crash of 1997 and the LTCM crisis of 1998 brought the short-term VFTSE to levels exceeding 50%, and at the onset of the banking crisis the VFTSE exceeded 80% on a few days. However, during the trending equity markets of the post crisis period the VFTSE has mysteriously failed to reach those previous heights, despite the mounting uncertainties in the global economy.[18]

Table 4 reports the first four moments of the empirical distribution of the GVSR and the AVSR*, again for maturities $30, 60, \ldots, 270$ calendar days. This is for daily data over the whole sample (top section) and separately for the Banking crisis period between September 2008 to March 2009 (lower section). The highest and most variable rate, on average, is the GVSR. This is due to the net upward Riemann sum bias, as demonstrated in Section 4. As expected, the bias is smaller on average over the entire sample than it is during the banking crisis when the option price distribution was extremely skewed. The term structure is quite flat over the whole sample, but decreasing during the crisis, again as expected. The skewness and kurtosis of the two rates are similar, both decreasing with maturity because the volatility term structure becomes flatter as we move up the curve. During the banking crisis the skewness and kurtosis are much lower, being standardised higher moments, because the VSRs were so variable at that time.

Figure 6 depicts the difference between the GVSR and the AVSR* over the entire sample, in grey. Because of the variability, we also show a smoothed version of the difference, in black.[19] It is remarkable that the variability in their difference increases noticeably after the

[17] At this granularity differences between the GVSR and the AVSR* are not worthy of comment beyond the descriptive statistics in Table 4. Here we present the AVSR* for the FTSE 100.

[18] Indeed the VVIX, the volatility of the VIX has (at the time of writing) reached and all time high of 160%. Further discussion of this topic is, unfortunately, not relevant to the subject of this paper.

[19] Given the high variability in the difference in rates, especially since the banking crisis, we smooth this difference using an exponentially weighted moving average with smoothing constant 0.97.

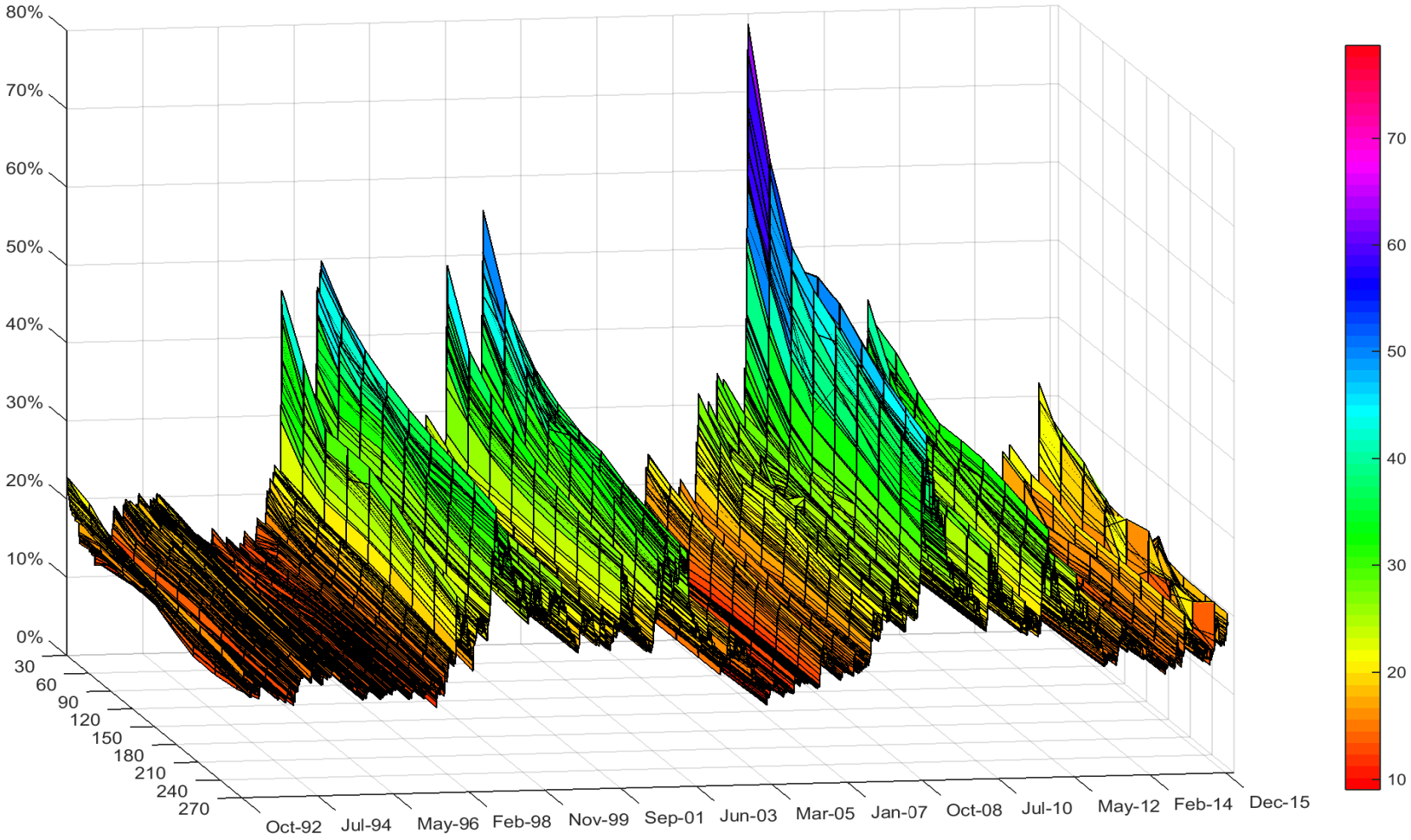

Figure 5: VFTSE Term-Structure Time Series
The VFTSE term structure for maturities from 30 to 270 days between 12 October 1992 and 22 December 2015.

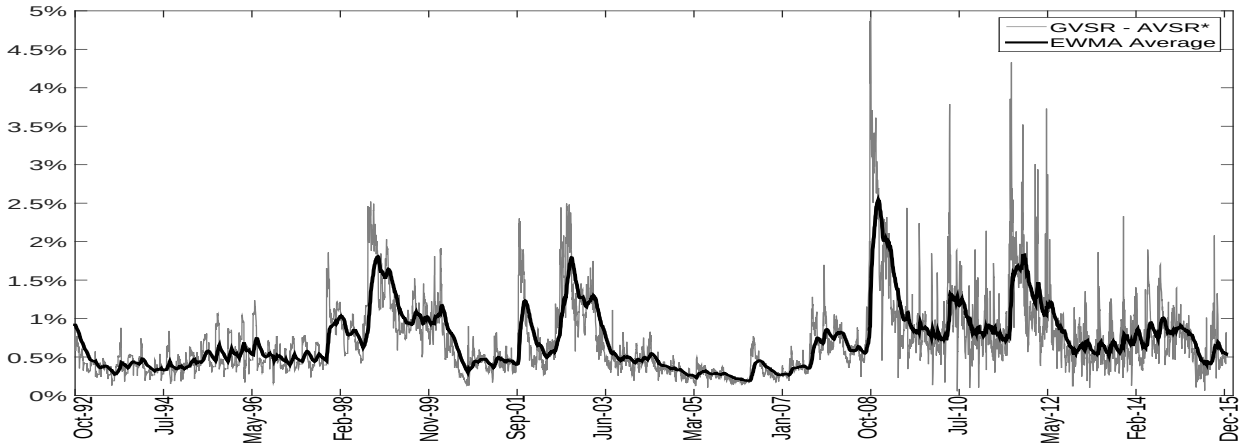

Figure 6: GVSR − AVSR*
The grey line shows the difference between the GVSR and the AVSR* between October 1992 and December 2015. The black line shows a smoothed time series based on an exponentially weighted moving average with smoothing constant 0.97.

banking crisis period. Clearly, the relatively high weights that the GVSR calculation places on deep OTM put options is influencing their index, because it is precisely these options that become less liquid and have more unreliable prices during periods of high uncertainty.

The essential difference between the two formulae lies in their weighting on OTM puts, which have a higher weighting in the standard VSR used by the CBOE (and other exchanges). The excessive variability that is evident in the difference in rates, since the banking crisis, coincides with a highly uncertain period in equity markets, when trading on OTM puts becomes extremely volatile. This would also explain the unusually high volatility in the VVIX index, which is derived from vanilla options on the VIX index in the same way as the VIX is derived from vanilla options on the S&P 500 index, i.e. using (11). High levels of the VVIX indicate higher prices for VIX options due to greater uncertainty in the the VIX. Its record high at the time of writing was almost 170%, when the S&P 500 index fell 11% on 24 August 2015.

6.2 Comparison of 30-day VSRs in the Banking Crisis

Figure 7 shows three daily time series plots just during the banking crisis, i.e. the 6 month period September 2008 to end March 2009.[20] The upper one depicts three 30-day FTSE 100 variance swap rates: the GVSR (red), its approximation AVSR* (blue) and the BNP Paribas 30-day swap rate (black). The middle graph depicts the difference BNP – GVSR and the lower one the difference GVSR – AVSR*.

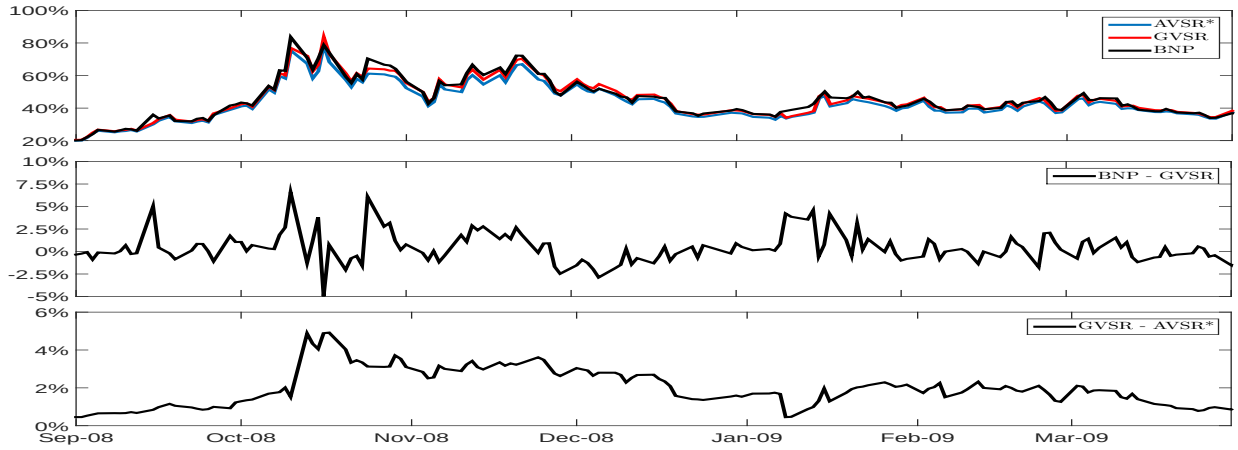

Figure 7: Model and Market VSRs
A comparison of the BNP Paribas 30-day VSR with the GVSR the AVSR*, during the banking crisis between September 2008 and March 2009. The upper graph depicts the rates themselves, and the differences (BNP – GVSR) and (GVSR – AVSR*) are shown in the two lower graphs.

The rates rose rapidly from 20% to about 140% during October 2008, falling again but remaining very high and variable until the end of the year. Still, they remained above 40% until the end of March 2009. The middle graph shows by how much the BNP rate exceeds the GVSR, exhibiting several spikes of 5% or more, as previously observed by Ait-Sahalia et al. [2014]. This demonstrates the negative jump and discretisation biases which can be significant during volatile periods, as argued in the introduction. Market rates occasionally dipped up to 5% below their fair-values during the initial part of the crises, possibly because liquidity issues in OTM puts would make replication portfolios more highly priced and therefore increase the GVSR. By the same token, the GVSR exceeded the AVSR* by about

[20] Until the banking crisis the divergence between the market rates and their fair-values rarely exceeded 2%. Most of the time the market rates were above their fair values, with the arithmetic approximate rates being the lowest, as before.

3% on average, during the six-month sample period. On a few days in October 2008 the GVSR quote was around 5% greater than the AVSR*. As demonstrated in Section 4.2, and previously by Jiang and Tian [2007], the positive Riemann-sum bias can be very significant indeed during crisis periods. Such a great divergence between the two rates may also be due to another feature not focussed on until this paper, which is the extra reliance of the standard swap rate formula on illiquid options for which reliable prices are difficult to find.

6.3 Term Structures for Arithmetic Skewness and Kurtosis Swap Rates

In this section we depict time series of term structures of some fair-value arithmetic higher-moment swap rates, i.e. higher moments of the implied distribution at a variety of maturities. These are: the arithmetic third-moment swap rate (A3SR), and fourth-moment rate (A4SR); and the equivalent swap rates for skewness (ASSR) and (excess) kurtosis (AKSR). These are implemented via replication portfolios for the centralised moments of the risk neutral density for S_T. Following derivations in the Appendix we compute the option price integrals $\mathcal{I}_n = \int_0^\infty k^n \, Q\left(k,T\right) \, dk$ and then set: $\text{A3SR} = 2\Big(3\mathcal{I}_1 - 3F_{t,T}\mathcal{I}_0 + \left(F_{t,T} - k_0\right)^3\Big)$, and $\text{A4SR} = 3\Big(4\mathcal{I}_2 - 8F_{t,T}\mathcal{I}_1 + 4F_{t,T}^2\mathcal{I}_0 - \left(F_{t,T} - k_0\right)^4\Big)$. Standardizing these yields the skewness swap rate

$$\text{ASSR} = \text{AVSR}^{-3/2}\text{A3SR}, \tag{14}$$

and

$$\text{AKSR} = \text{AVSR}^{-2}\text{A4SR} - 3, \tag{15}$$

the excess kurtosis swap rate.

Table 5 reports descriptive statistics for the FTSE 100 implied higher moments. As before we exhibit two tables, one for the entire sample and one for the banking crisis between 1 September 2008 and 31 March 2009. These results confirm that the FTSE 100 equity index returns are negatively skewed, less so as maturity increases. The heavier left tail in the short-term FTSE 100 forward implied distribution indicates investor's fear of a sudden correction during trending markets. However, during the banking crisis the implied skewness

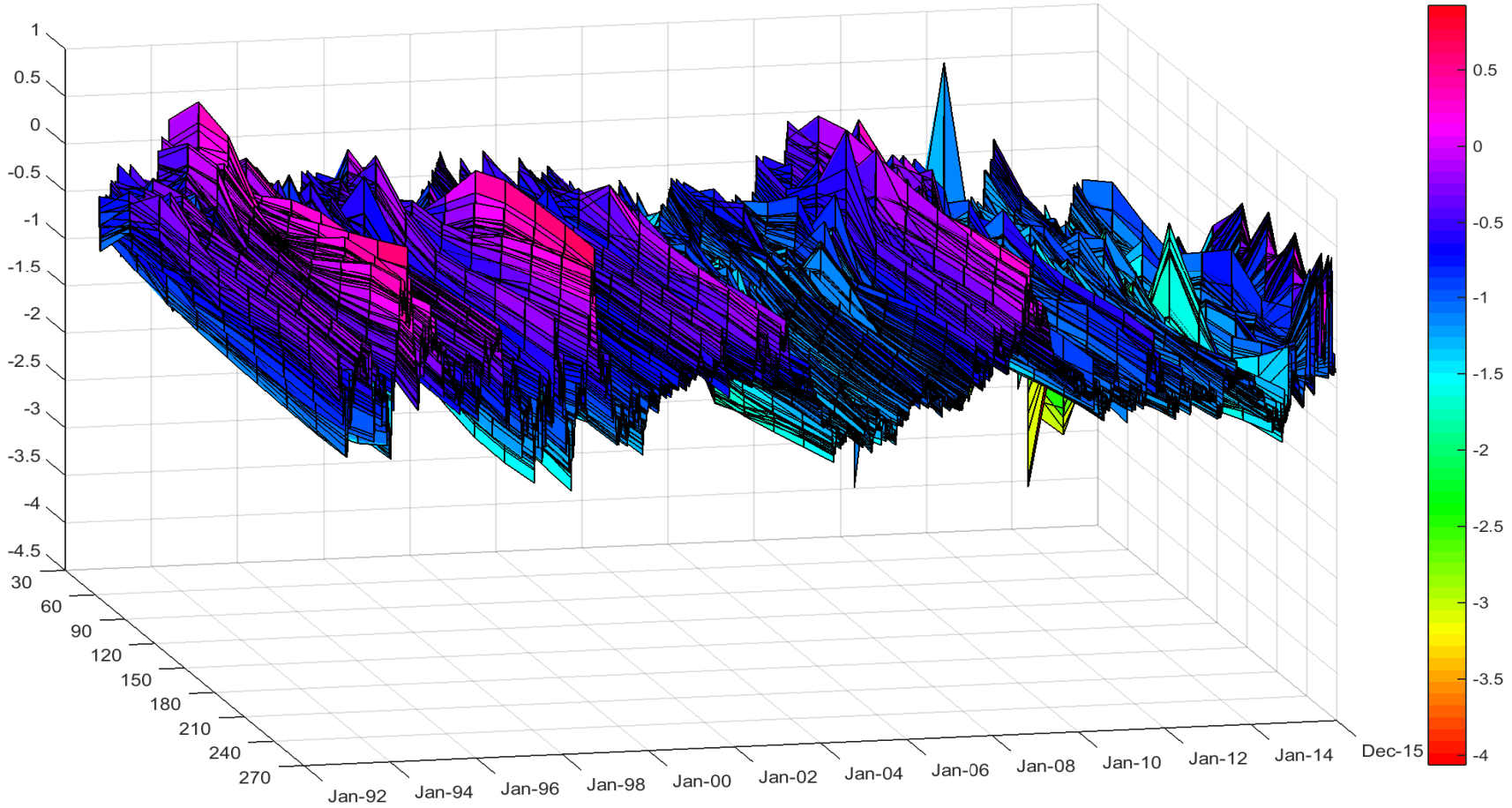

Figure 8: ASSR Term-Structure Time Series
The FTSE 100 ASSR term structure for maturities from 30 to 270 days between 12 October 1992 and 22 December 2015.

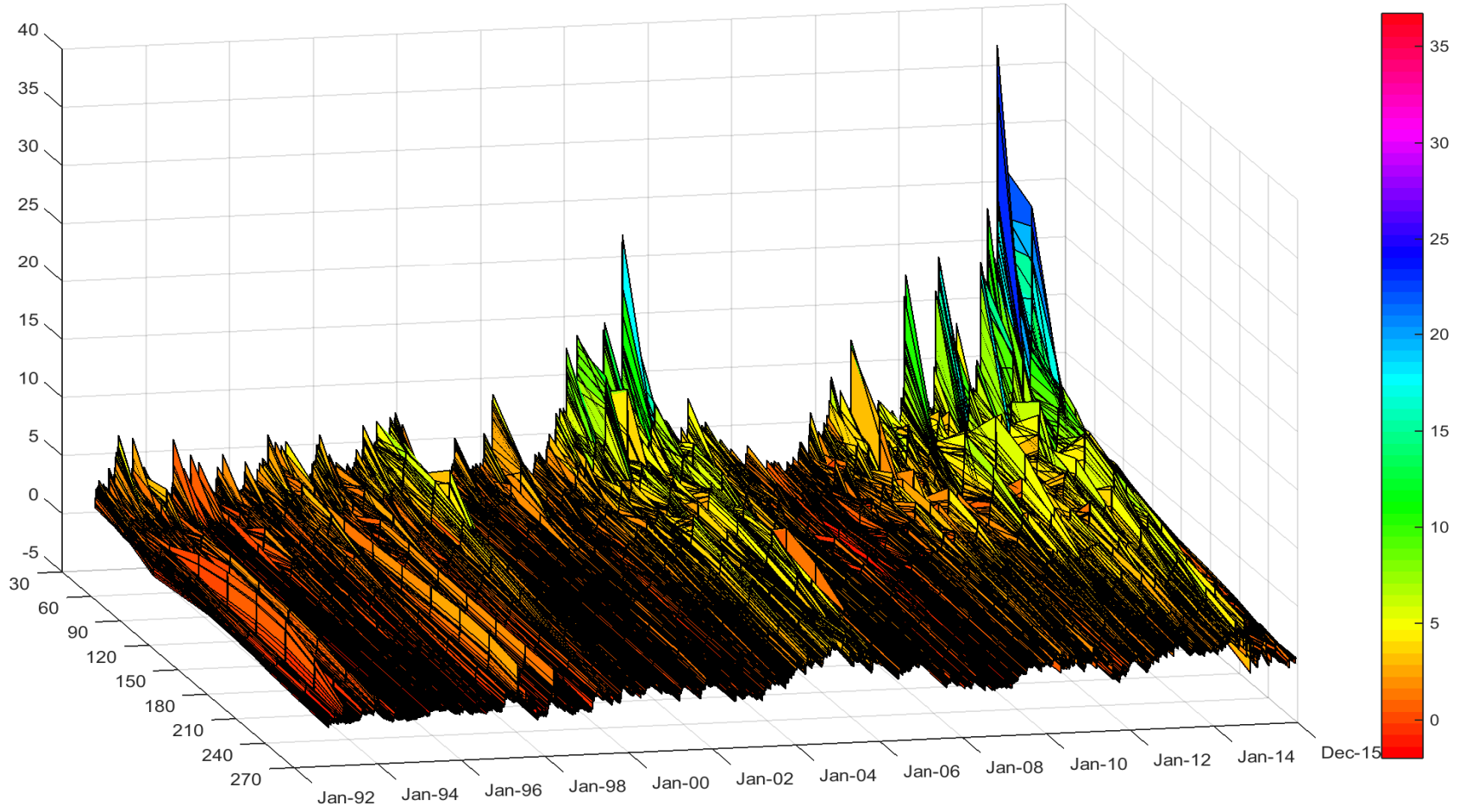

Figure 9: AKSR Term-Structure Time Series
The FTSE 100 AKSR term structure for maturities from 30 to 270 days between 12 October 1992 and 22 December 2015.

decreases, and the implied excess kurtosis is only slightly positive in the short-term, being negative further up the curve.

Figure 8 depicts the entire ASSR term structure curves for the FTSE 100, daily. Crises periods when the implied skewness becomes high and positive are notable in 1997 and 1998, with the Asian property crisis and the enormous losses made by LTCM, respectively. Of course, this also occurs at the onset of the banking crisis in September 2008. While the variance term structure in Figure 5 has a persistent contango pattern, most evident in recent years, the skew term structure in Figure 5 is relatively flat but extremely variable, especially since the banking crisis when it fluctuates even over term in a less correlated manner.

Similarly, Figure 9 depicts the term structure for (excess) implied kurtosis of the FTSE 100. By contrast with the lower-moment swap rates, the implied excess kurtosis is negligible except at very near-term maturities. The implied density has exceedingly heavy tails during the banking crisis. But since mid 2012 it has, rather disconcertingly, been even higher on many days, frequently reaching values in excess of 20. At these times excess kurtosis is also significant a longer maturities along the term structure.

6.4 Empirical Correlations

Finally, we analyse the correlations between the daily changes in the implied variance of the price distribution and the corresponding changes in the higher central moments that are captured by A3SR and A4SR.[21] Figure 10 reports the results, based on the entire sample (left) and separately over the banking crisis period (right). The potential to differentiate variance risk by entering arithmetic higher-moment swaps will be evidenced by low, even negative, values for these correlations.

Predictably, since they both reflect the range in the implied density, there is a positive correlation between the variance swap rate AVSR and the kurtosis swap rate AKSR, at all maturities. By contrast, the correlations between the skewness rate ASSR and the other

[21] Correlations between AVSR and the standardized higher-moment rates ASSR and AKSR are less informative because they are influenced by the use of AVSR to standardize these moments. As such, they are obviously negative and, by the same token, the ASSR and AKSR have a high positive correlation.

two are typically negative, at least at shorter maturities. During the banking crisis, shown in the right-hand panel of Figure 10, the AVSR correlations increase: only marginally for the AVSR-AKSR, but the correlations between the AVSR and ASSR increase on by about 0.5, in absolute terms, on average over the whole term structure. Now they are almost all positive, and short-term AVSRs have a high positive correlation with AVSRs at the longer end of the term structure.

Over the entire sample the 30-day AVSR-A3SR correlation is -0.45 and during the crisis period it is $+0.19$. Hence, the correlation between the variance and skewness 30-day swap rates still remains low during the banking crisis. We conclude that skewness swaps represent quite a different source for return than variance risk.

7 Conclusions

This paper examines the fair value of an arithmetic variance swap for realised variance defined as the sum of the squared price changes rather than the sum of squared changes of their logarithms. It is model-free in the sense that it only requires the forward price to follow a martingale, and a derivation using the moment generating function of the risk-neutral price density yields fair-values for the implied variance and higher moments of the forward price. As such it is directly applicable to pricing variance swaps on spreads, or interest rates or electricity prices any other instrument which can become zero or negative.

This approach has some advantages over the fair-value variance swap formula used by exchanges to price standard variance swaps. The new definition for realised variance satisfies the aggregation property introduced by Bondarenko [2014] and Neuberger [2012]. As such its fair value does not suffer from discrete-monitoring or jump biases, unlike that for the standard realised variance. Also, the standard variance swap rate requires weighting of option prices by the inverse of the square of their strike, making the resulting integration especially sensitive to liquidity risk on low strike options, and errors from their frequently stale prices. By contrast, the arithmetic variance swap rate uses an equally-weighted integral

over option prices.

A numerical study analyses the truncation and strike-discretisation biases introduced by both formulae, at both 30-day and 180-day swap maturities. We conclude that one should not use one fair-value to approximate the other because the errors are considerable.

Using 23 years of daily data on FTSE 100 options, we construct constant-maturity investable empirical data spanning 23 years, free from artefactual distortions such as varying maturity or autocorrelation. We apply Hermite spline interpolation over variance to obtain arbitrage-free constant-maturity option prices. We compute the fair value arithmetic swap rate using an analytic formula for the coefficients of the cubic splines. We also compute the standard variance swap rate, following the numerical methods employed by the CBOE, and then compare this empirically with the approximate rate for a standard variance swap derived from the arithmetic swap rate.

We observe substantial empirical differences between these swap rates during turbulent market periods when the biases in variance swap rates are particularly pronounced. Nevertheless, the implied legs of the two variance swaps are very highly correlated. The average correlation across the term structures for the daily changes in standard and arithmetic rates is 83%, being only slightly higher at short maturities and decreasing as they move up the curve. The realised legs of the two swaps have also been extremely highly correlated: over the same sample for the FTSE 100 futures, the daily changes in realised variance have a correlation which also averaged 83% over the term structure, and again it decreases only slightly with maturity.[22] Thus, variance swap issuers would be capturing very similar premia by switching from standard to arithmetic variance swaps. The unbiased, more flexible and more broadly applicable 'arithmetic' definition for realised variance has many qualities superior to the standard definition.

Finally, we replicate the term structure for arithmetic third- and fourth-moment swap rates, observing their features. Correlations between the 30-day implied variance and third

[22]Correlations between the levels of the two implied/realised legs are, of course, far higher, at 97.5% on average over our sample.

moment are low and negative, overall, although they do rise during turbulent periods. Nevertheless, variance and third-moment risks do appear to capture different sources of return.

References

Y. Ait-Sahalia, M. Karaman, and L. Mancini. The term structure of variance swaps and risk premia. *Working Paper*, 2014. URL `http://papers.ssrn.com/sol3/Papers.cfm?abstract_id=2136820`.

C. Alexander and J. Rauch. Model-free discretisation-invariant swap contracts. *arXiv preprint arXiv:1602.00235*, 2016.

C. Alexander, J. Kapraun, and D. Korovilas. Trading and investing in volatility products. *Financial Markets, Institutions & Instruments*, 24(4):313–347, 2015.

G. Bakshi, N. Kapadia, and D. Madan. Stock return characteristics, skew laws, and the differential pricing of individual equity options. *Review of Financial Studies*, 16(1):101–143, 2003.

C. Bernard, Z. Cui, and D. Mcleish. Convergence of the discrete variance swap in time-homogeneous diffusion models. *Quantitative Finance Letters*, 2(1):1–6, 2014.

F. Black and M. Scholes. The pricing of options and corporate liabilities. *The Journal of Political Economy*, 81(3):637–654, 1973.

R. Bliss and N. Panigirtzoglou. Option-implied risk aversion estimates. *The Journal of Finance*, 59(1):407–446, 2004.

O. Bondarenko. Variance trading and market price of variance risk. *Journal of Econometrics*, 180(1):81–97, 2014.

D. Breeden and R. Litzenberger. State contingent prices implicit in option prices. *Journal of Business*, 51:621–651, 1978.

M. Britten-Jones and A. Neuberger. Option prices, implied price processes, and stochastic volatility. *The Journal of Finance*, 55(2):839–866, 2000.

M. Broadie and A. Jain. The effect of jumps and discrete sampling on volatility and variance swaps. *International Journal of Theoretical and Applied Finance*, 11(8):761–979, 2008.

P. Carr and R. Lee. Robust replication of volatility derivatives. *Unpublished paper: Courant Institute, NYU*, 2003.

P. Carr and R. Lee. Volatility derivatives. *Annual Review of Financial Economics*, 1:1–21, 2009.

P. Carr and D. Madan. Towards a theory of volatility trading. *Working Paper*, 2002. URL `http://www.math.nyu.edu/research/carrp/papers/pdf/twrdsfig.pdf`.

J. Clark. Return to variance? *Risk Magazine*, 23(2):online, 2010.

C. De Boor. *A Practical Guide to Splines*. Springer Verlag, 2001.

K. Demeterfi, E. Derman, M. Kamal, and J. Zou. A guide to volatility and variance swaps. *Journal of Derivatives*, 6(4):9–32, 1999.

J. Du and N. Kapadia. Tail and volatility indices from option prices. *Working Paper, University of Massachusetts.*, 2012.

F. Fritsch and R. Carlson. Monotone piecewise cubic interpolation. *SIAM Journal on Numerical Analysis*, 18:238–246, 1980.

P. Friz and J. Gatheral. Pricing volatility derivatives as inverse problem. *Quantitative Finance*, 5(6):531–542, 2005.

J. Gatheral. *The Volatility Surface: A Practitioner's Guide*. Wiley, 2006.

S. Heston. A closed-form solution for options with stochastic volatility with applications to bond and currency options. *Review of Financial Studies*, 6(2):327–343, 1993.

R. Jarrow, Y. Kchia, M. Larsson, and P. Protter. Discretely sampled variance and volatility swaps versus their continuous approximations. *Finance and Stochastics*, 17:305–324, 2013.

G.J. Jiang and Y.S. Tian. The model-free implied volatility and its information content. *Review of Financial Studies*, 18(4):1305, 2005.

G.J. Jiang and Y.S. Tian. Extracting model-free volatility from option prices: An examination of the VIX index. *Journal of Derivatives*, 14(3):35, 2007.

JPMorgan. Variance Swaps. *European Equity Derivatives Research*, 2006.

A. Kaeck and C. Alexander. Stochastic volatility jump-diffusions for european equity index dynamics. *European Financial Management*, 19(3):470–496, 2013.

E. Konstantinidi and G. Skiadopoulos. How does the market variance risk premium vary over time? evidence from s&p 500 variance swap investment returns. *Journal of Banking and Finance*, 62,:62–75, 2016.

A. Kostakis, N. Panigirtzoglou, and G. Skiadopoulos. Market timing with option-implied distributions: A forward-looking approach. *Management Science*, 57(7):1231–1249, 2011.

I. Martin. Simple variance swaps. *Working Paper*, 2013. URL `http://personal.lse.ac.uk/martiniw/simple%20variance%20swaps%20latest.pdf`.

P. Mueller, A. Vedolin, and Y-M. Yen. Bond variance risk premia. *Working Paper, London School of Economics, SSRN: 1787478*, 2013.

A. Neuberger. The log contract. *The Journal of Portfolio Management*, 20(2):74–80, 1994.

A. Neuberger. Realized skewness. *Review of Financial Studies*, 25(11):3423–3455, 2012.

M. Neumann and G. Skiadopoulos. Predictable dynamics in higher order risk-neutral moments: Evidence from the s&p 500 options. *Journal of Financial and Quantitative Analysis*, 48(3):947–977, 2012.

N. Panigirtzoglou and G. Skiadopoulos. A new approach to modeling the dynamics of implied distributions: Theory and evidence from the s&p 500 options. *Journal of Banking & Finance*, 28(7):1499–1520, 2004.

L. Rompolis and E. Tzavalis. Retrieving risk-neutral moments from option prices. *Working Paper*, 2013. URL `http://papers.ssrn.com/sol3/papers.cfm?abstract_id=936670`.

S.E. Shreve. *Stochastic Continuous Calculus For Finance II: Continuous-time Models*. Springer, 2004.

8 Appendix

8.1 Arithmetic Higher-Moment Swap Rates

The risk-neutral moment generating function (MGF) for S_T is defined as $\mathcal{M}_{S_T}(\lambda) = \mathbb{E}\left[\exp(\lambda S_T)\right]$. The n^{th} moment of the distribution of S_T is obtained by taking the n^{th} derivative of the MGF with respect to λ and setting $\lambda = 0$. We start with the well-known result of Breeden and Litzenberger [1978], writing

$$\mathcal{M}_{S_T}(\lambda) = \int_{k=0}^{\infty} e^{\lambda k} \frac{\partial^2 \tilde{C}(k,T)}{\partial k^2} dk.$$

Next we use the following properties of call option prices:

$$\lim_{k\to 0} \tilde{C}(k) = S_T, \lim_{k\to+\infty} \tilde{C}(k) = 0, \lim_{k\to 0} \frac{\partial \tilde{C}(k)}{\partial k} = -1 \text{ and } \lim_{k\to+\infty} \frac{\partial \tilde{C}(k)}{\partial k} = 0.$$

Integrating by parts twice yields:

$$\begin{aligned}
\mathcal{M}_{S_T}(\lambda) &= e^{\lambda k} \left.\frac{\partial \tilde{C}(k,T)}{\partial k}\right|_0^{\infty} - \lambda \int_{k=0}^{\infty} e^{\lambda k} \frac{\partial \tilde{C}(k,T)}{\partial k} dk \\
&= e^{\lambda(+\infty)} \left.\frac{\partial \tilde{C}(k,T)}{\partial k}\right|_{k=+\infty} - e^{\lambda\cdot 0} \left.\frac{\partial \tilde{C}(k,T)}{\partial k}\right|_{k=0} - \lambda \int_{k=0}^{+\infty} e^{\lambda k} \frac{\partial \tilde{C}(k,T)}{\partial k} dk \\
&= 0 - (-1) - \lambda \int_{k=0}^{+\infty} e^{\lambda k} \frac{\partial \tilde{C}(k,T)}{\partial k} dk \\
&= 1 - \lambda e^{\lambda k} \tilde{C}(k,T)\Big|_0^{\infty} + \lambda^2 \int_{k=0}^{\infty} e^{\lambda k} \tilde{C}(k,T)\, dk \\
&= 1 - \lambda e^{\lambda(+\infty)} \tilde{C}(k,T)\Big|_{k=+\infty} + \lambda e^{\lambda\cdot 0} \tilde{C}(k,T)\Big|_{k=0} + \lambda^2 \int_{k=0}^{+\infty} e^{\lambda k} \tilde{C}(k,T)\, dk \\
&= 1 - 0 + \lambda \mathbb{E}[S_T] + \lambda^2 \int_{k=0}^{+\infty} e^{\lambda k} \tilde{C}(k,T)\, dk \\
&= 1 + \lambda F_{t,T} + \lambda^2 \int_{k=0}^{\infty} e^{\lambda k} \tilde{C}(k,T)\, dk,
\end{aligned}$$

i.e. the MGF is:

$$\mathcal{M}_{S_T}(\lambda) = 1 + \lambda F_{t,T} + \lambda^2 \int_{k=0}^{\infty} e^{\lambda k} \tilde{C}(k,T)\, dk. \tag{16}$$

Thus

$$\begin{aligned}
\mathbb{E}\left[S_T^n\right] &= \left. \frac{d^n \mathcal{M}_{S_T}(\lambda)}{d\lambda^n} \right|_{\lambda=0} \\
&= \left. \begin{array}{l} F_{t,T} 1_{\{n=1\}} + n(n-1) \int_{k=0}^{\infty} e^{\lambda k} k^{n-2} C(k)\, dk + 2n\lambda \int_{k=0}^{\infty} e^{\lambda k} k^{n-1} C(k)\, dk + \\ \lambda^2 \int_{k=0}^{\infty} e^{\lambda k} k^n C(k)\, dk \end{array} \right|_{\lambda=0}
\end{aligned}$$

For replication in terms of OTM option prices alone we use the put-call parity relationship:

$$\begin{aligned}
\mathcal{M}_{S_T}(\lambda) &= 1 + \lambda F_{t,T} + \lambda^2 \int_{k=0}^{\infty} e^{\lambda k} \tilde{C}(k,T)\, dk \\
&= 1 + \lambda F_{t,T} + \lambda^2 \int_{k=0}^{k_0} e^{\lambda k} \left[F_{t,T} - k + \tilde{P}(k,T)\right] dk + \int_{k=k_0}^{\infty} e^{\lambda k} \tilde{C}(k,T)\, dk \\
&= 1 + \lambda F_{t,T} + \lambda F_{t,T}\left(e^{\lambda k_0} - 1\right) - \left(1 + e^{\lambda k_0}(\lambda k_0 - 1)\right) + \lambda^2 \int_{k=0}^{k_0} e^{\lambda k} \tilde{P}(k,T)\, dk \\
&\quad + \int_{k=k_0}^{\infty} e^{\lambda k} \tilde{C}(k,T)\, dk.
\end{aligned}$$

Hence, an alternative form of (7) is

$$\mathcal{M}_{S_T}(\lambda) = e^{\lambda k_0}(1 + \lambda F_t - \lambda k) + \lambda^2 \left(\int_{k=0}^{\infty} e^{\lambda k} \tilde{\mathcal{Q}}(k,T)\, dk \right), \tag{17}$$

where

$$\tilde{\mathcal{Q}}(k,T) = \begin{cases} \tilde{P}(k,T|\, S_t,t) & k < S_t^*, \\ \tilde{C}(k,T|\, S_t,t) & k \geq S_t^*. \end{cases} \tag{18}$$

Note that one possible discretisation of (16) is

$$\mathcal{M}_{S_T}(\lambda) = e^{\lambda F_T} + \lambda^2 e^{r(T-t)} \sum_i e^{\lambda k_i} \tilde{\mathcal{Q}}(k_i,T)\, \Delta k_i. \tag{19}$$

Based on the above representation we have:

$$\begin{aligned}\mu_{t,T}=\mathbb{E}\left(S_{_T}\right) &= \left.\frac{d\mathcal{M}_{S_{_T}}\left(\lambda\right)}{d\lambda}\right|_{\lambda=0}=F_{t,T}\\ &= \left.\begin{array}{l} e^{\lambda k_0}\left(F_{t,T}-k_0\right)+e^{\lambda k_0}k_0\left(1+\lambda F_{t,T}-\lambda k\right)+2\lambda\int\limits_{k=0}^{\infty}e^{\lambda k}\tilde{Q}\left(k,T\right)dk \\ +\lambda^2\int\limits_{k=0}^{\infty}e^{\lambda k}k\tilde{Q}\left(k,T\right)dk \end{array}\right|_{\lambda=0}\end{aligned}$$

The second central moment is:

$$\begin{aligned}\mathbb{E}\left[S_{_T}^2\right] &= \left.\frac{d^2\mathcal{M}_{S_{_T}}\left(\lambda\right)}{d\lambda^2}\right|_{\lambda=0}\\ &= \left.\begin{array}{l} 2e^{\lambda k_0}\left(F_{t,T}-k_0\right)k_0+e^{\lambda k_0}k_0^2\left(1+\lambda\left(F_{t,T}-k_0\right)\right)+2\int\limits_{k=0}^{\infty}e^{\lambda k}\tilde{Q}\left(k,T\right)dk \\ +4\,\lambda\int\limits_{k=0}^{\infty}e^{\lambda k}k\tilde{Q}\left(k,T\right)dk+\lambda^2\int\limits_{k=0}^{\infty}e^{\lambda k}k^2\tilde{Q}\left(k,T\right)dk \end{array}\right|_{\lambda=0}\\ &= 2\left(F_{t,T}-k_0\right)k_0+k_0^2+2\int\limits_{k=0}^{\infty}\tilde{Q}\left(k,T\right)dk.\end{aligned}$$

Thus,

$$\begin{aligned}\sigma_{t,T}^2 &= 2\left(F_{t,T}-k_0\right)k_0+k_0^2+2\int\limits_{k=0}^{\infty}\tilde{Q}\left(k,T\right)dk-F_{t.T}^2\\ &= 2\int\limits_{k=0}^{\infty}\tilde{Q}\left(k,T\right)dk-\left(F_{t,T}-k_0\right)^2. \qquad (20)\end{aligned}$$

The third central moment is:

$$\begin{aligned}\mathbb{E}\left[S_{_T}^3\right] &= \left.\frac{\partial^3\mathcal{M}_{S_{_T}}\left(\lambda\right)}{\partial\lambda^3}\right|_{\lambda=0}\\ &= \left.\begin{array}{l} 3e^{\lambda k_0}k_0^2\left(F_{t,T}-k_0\right)+e^{\lambda k}k_0^3\left(1+\lambda F_{t,T}-\lambda k_0\right)+6\int\limits_{k=0}^{\infty}e^{\lambda k}k\tilde{Q}\left(k,T\right)dk+ \\ 6\lambda\int\limits_{k=0}^{\infty}e^{\lambda k}k^2\tilde{Q}\left(k,T\right)dk+\lambda^2\int\limits_{k=0}^{\infty}e^{\lambda k}k^3\tilde{Q}\left(k,T\right)dk \end{array}\right|_{\lambda=0}\\ &= 3\left(F_{t,T}-k_0\right)k_0^2+k_0^3+6\int\limits_{k=0}^{\infty}k\tilde{Q}\left(k,T\right)dk.\end{aligned}$$

This yields the price skewness:

$$\tau_{t,T} = 2^{-1/2} \frac{\left((F - k_0)^3 - 3F_{t,T} \int_{k=0}^{\infty} \tilde{Q}(k,T)\, dk + 3 \int_{k=0}^{\infty} k\tilde{Q}(k,T)\, dk \right)}{\left(\int_{k=0}^{\infty} \tilde{Q}(k,T)\, dk - (F_{t,T} - k_0)^2 \right)^{3/2}}. \tag{21}$$

Finally, the fourth central moment is:

$$\begin{aligned}
\mathbb{E}\left[S_T^4\right] &= \left. \frac{\partial^4 \mathcal{M}_{S_T}(\lambda)}{\partial \lambda^4} \right|_{\lambda=0} \\
&= \left. \begin{array}{l} 4e^{\lambda k_0} k_0^3 (F_{t,T} - k_0) + e^{\lambda k} k_0^4 (1 + \lambda F_{t,T} - \lambda k_0) + 12 \int_{k=0}^{\infty} e^{\lambda k} k^2 \tilde{Q}(k,T)\, dk \\ +8\lambda \int_{k=0}^{\infty} e^{\lambda k} k^3 \tilde{Q}(k,T)\, dk + \lambda^2 \int_{k=0}^{\infty} e^{\lambda k} k^4 \tilde{Q}(k,T)\, dk \end{array} \right|_{\lambda=0} \\
&= 4(F_{t,T} - k_0) k_0^3 + k_0^4 + 12 \int_{k=0}^{\infty} k^2 \tilde{Q}(k,T)\, dk.
\end{aligned}$$

Thus the price kurtosis is:

$$\kappa_{t,T} = -3 \frac{(F_{t,T} - k_0)^4 - 4F_{t,T} \int_{k=0}^{\infty} \tilde{Q}(k,T)\, dk + 8F_{t,T} \int_{k=0}^{\infty} k\tilde{Q}(k,T)\, dk - 4 \int_{k=0}^{\infty} k^2 \tilde{Q}(k,T)\, dk}{2 \int_{k=0}^{\infty} \tilde{Q}(k,T)\, dk - (F_{t,T} - k_0)^2}$$

Summarising, we can set $\mathcal{I}_n = \int_0^\infty k^n Q(k,T)\, dk$ to derive succinct expressions for the first four moments of S_T, viz.:

$$\begin{aligned}
\sigma_{t,T}^2 &= 2\mathcal{I}_0 - (F_{t,T} - k_0)^2, \\
\tau_{t,T} &= 2\Big(3\mathcal{I}_1 - 3F_{t,T}\mathcal{I}_0 + (F_{t,T} - k_0)^3\Big)\sigma_{t,T}^{-3}, \\
\kappa_{t,T} &= 3\Big(4\mathcal{I}_2 - 8F_{t,T}\mathcal{I}_1 + 4F_{t,T}^2\mathcal{I}_0 - (F_{t,T} - k_0)^4\Big)\sigma_{t,T}^{-4}.
\end{aligned}$$

Only three price integrals are required and, as the order n of the moment increases these integrals place decreasing relative weight on OTM puts.

8.2 An Alternative GVSR, Bakshi et al. [2003]

Using a fourth-order Taylor approximation of the moment generating function of the underlying price at maturity T, Bakshi et al. [2003] derive the following approximate expression for the risk-neutral expected value of the contract which pays the squared log return:

$$V_{t,T} = 2e^{r(T-t)} \int_0^\infty \left(1 + \ln\left[\frac{S^*_{t,T}}{k}\right]\right) \frac{\mathcal{Q}_t(k,T)}{k^2}\, dk.$$

This yields a second formula for the fair-value VSR, viz.

$$\tilde{K}_{t,T} = (T-t)^{-1}\left(V_{t,T} - \mu^2_{t,T}\right), \tag{22}$$

where $\mu_{t,T}$ is the risk-neutral expected value of the log return.

Assuming a jump-free continuous martingale underlying price process, Britten-Jones and Neuberger [2000] shows how the risk-neutral expectation of the quadratic variation between two finite time intervals can be estimated using observable option prices. Both Carr and Madan [2002] and Gatheral [2006] express this expectation as the first moment of the log return. Carr and Lee [2003] and Jiang and Tian [2005] generalise this to different price process dynamics, the latter showing that (3) is identical to the unconditional centralised second moment of the log returns, as derived in (22). In the same vein, Rompolis and Tzavalis [2013] derive the risk-neutral characteristic function of any random pay-off defined on a semi-martingale and show that (22) may be derived from this when the pay-off is the log return. In the absence of jumps, the two VSRs are approximately equivalent.

BSM Model															
		True AVSR		GVSR* Errors		AVSR Errors		GVSR* Errors		AVSR Errors		GVSR* Errors		AVSR Errors	
				k=5:0.1:500				k=25:0.1:175				k=5:1:500			
S0	**V0**	**T=30**	**T=180**	**T=30**	**T=180**	**T=30**	**T=180**	**T=30**	**T=180**	**T=30**	**T=180**	**T=30**	**T=180**	**T=30**	**T=180**
80	20	4.623	11.371	-0.08%	-0.50%	0.00%	0.00%	-0.08%	-0.50%	0.00%	0.00%	0.31%	-0.43%	0.39%	0.06%
80	40	9.268	23.088	-0.33%	-1.99%	0.00%	0.00%	-0.33%	-2.01%	0.00%	-0.08%	-0.24%	-1.98%	0.10%	0.02%
80	60	13.961	35.527	-0.75%	-4.46%	0.00%	0.00%	-0.75%	-4.78%	0.00%	-1.66%	-0.71%	-4.46%	0.04%	0.01%
100	20	5.778	14.213	-0.08%	-0.50%	0.00%	0.00%	-0.08%	-0.50%	0.00%	0.00%	0.17%	-0.46%	0.25%	0.04%
100	40	11.586	28.859	-0.33%	-1.99%	0.00%	0.00%	-0.33%	-2.21%	0.00%	-0.78%	-0.27%	-1.98%	0.06%	0.01%
100	60	17.451	44.409	-0.75%	-4.46%	0.00%	0.00%	-0.75%	-5.66%	-0.01%	-4.97%	-0.72%	-4.46%	0.03%	0.00%
120	20	6.934	17.056	-0.08%	-0.50%	0.00%	0.00%	-0.08%	-0.53%	0.00%	-0.06%	0.09%	-0.47%	0.17%	0.03%
120	40	13.903	34.631	-0.33%	-1.99%	0.00%	0.00%	-0.34%	-3.33%	-0.01%	-3.49%	-0.29%	-1.99%	0.04%	0.01%
120	60	20.941	53.291	-0.75%	-4.47%	0.00%	-0.02%	-0.88%	-7.96%	-0.31%	-10.78%	-0.73%	-4.46%	0.02%	-0.02%

Table 2: Comparison of Truncation, Strike-Discretisation and Approximation Errors under GBM

Note: The relative error between the true variance swap rate for an arithmetic variance swap and the AVSR, and the error relative to the approximation GVSR*. Results are shown at two maturities, $T = 30$ and $T = 180$ and with 3 sets of strike price ranges. The first set of error results (labelled $k = [5 : 0.1 : 500]$) includes strikes starting at 5, ending at 500 with $dk = 0.1$ so that there is virtually no numerical error for AVSR. We do this so that the errors from using GVSR* can be isolated. The next four columns (9 – 12) isolate the effect of truncation error using set $k = [25 : 0.1 : 175]$ which includes strikes starting at 25, ending at 175 with $dk = 0.1$. The last set isolates the effect of discretisation error using set $k = [5 : 1 : 500]$ which includes strikes starting at 5, ending at 500 with $dk = 1$. All option prices are priced using the (Black and Scholes [1973]) model with $S = [80, 100, 120]$ and under low, mid and high volatility regimes of 20%, 40% and 60%, respectively.

Heston Model																	
				True GVSR		GVSR Errors		AVSR* Errors		GVSR Errors		AVSR* Errors		GVSR Errors		AVSR* Errors	
Parameters						k=5:0.1:500				k=25:0.1:175				k=5:1:500			
S	V0	θ	κ	T=30	T=180	T=30	T=180	T=30	T=180	T=30	T=180	T=30	T=180	T=30	T=180	T=30	T=180
80	20%	0.01	1	19.694	18.333	0.00%	0.00%	-2.28%	-10.60%	0.00%	-0.22%	-2.28%	-10.62%	0.40%	7.86%	-1.87%	-10.52%
80	20%	0.0625	1	20.227	21.165	0.00%	0.00%	-2.23%	-9.70%	0.00%	-0.20%	-2.23%	-9.72%	0.38%	-4.07%	-1.85%	-9.64%
80	20%	0.01	5	18.584	14.497	0.00%	0.00%	-2.13%	-7.09%	0.00%	-0.02%	-2.13%	-7.09%	0.45%	28.77%	-1.67%	-6.96%
80	20%	0.0625	5	21.000	23.289	0.00%	0.00%	-1.96%	-5.83%	0.00%	-0.02%	-1.96%	-5.83%	0.35%	-9.51%	-1.60%	-5.78%
100	20%	0.01	1	19.694	18.333	0.00%	0.00%	-2.28%	-10.60%	0.00%	-0.09%	-2.28%	-10.63%	0.26%	7.70%	-2.02%	-10.55%
100	20%	0.0625	1	20.227	21.165	0.00%	0.00%	-2.23%	-9.70%	0.00%	-0.08%	-2.23%	-9.73%	0.24%	-4.20%	-1.99%	-9.66%
100	20%	0.01	5	18.584	14.497	0.00%	0.00%	-2.13%	-7.09%	0.00%	0.00%	-2.13%	-7.09%	0.29%	28.56%	-1.83%	-7.01%
100	20%	0.0625	5	21.000	23.289	0.00%	0.00%	-1.96%	-5.83%	0.00%	-0.01%	-1.96%	-5.83%	0.23%	-9.63%	-1.73%	-5.80%
120	20%	0.01	1	19.694	18.333	0.00%	0.00%	-2.28%	-10.60%	0.00%	-0.09%	-2.28%	-10.76%	0.18%	7.62%	-2.10%	-10.56%
120	20%	0.0625	1	20.227	21.165	0.00%	0.00%	-2.23%	-9.70%	0.00%	-0.09%	-2.23%	-9.87%	0.17%	-4.27%	-2.06%	-9.67%
120	20%	0.01	5	18.584	14.497	0.00%	0.00%	-2.13%	-7.09%	0.00%	0.00%	-2.13%	-7.10%	0.20%	28.45%	-1.92%	-7.03%
120	20%	0.0625	5	21.000	23.289	0.00%	0.00%	-1.96%	-5.83%	0.00%	-0.02%	-1.96%	-5.86%	0.16%	-9.69%	-1.80%	-5.81%
80	50%	0.01	1	49.018	44.594	0.00%	0.00%	-1.89%	-9.30%	0.00%	-0.70%	-1.89%	-9.39%	0.06%	9.99%	-1.83%	-9.29%
80	50%	0.0625	1	49.234	45.831	0.00%	0.00%	-1.88%	-9.01%	0.00%	-0.71%	-1.88%	-9.11%	0.06%	7.49%	-1.82%	-9.00%
80	50%	0.01	5	45.418	31.324	0.00%	0.00%	-1.83%	-6.84%	0.00%	-0.09%	-1.83%	-6.85%	0.08%	45.10%	-1.75%	-6.81%
80	50%	0.0625	5	46.459	36.241	0.00%	0.00%	-1.77%	-5.98%	0.00%	-0.11%	-1.77%	-5.99%	0.07%	28.29%	-1.70%	-5.96%
100	50%	0.01	1	49.018	44.594	0.00%	0.00%	-1.89%	-9.30%	0.00%	-0.38%	-1.89%	-9.62%	0.04%	9.96%	-1.85%	-9.29%
100	50%	0.0625	1	49.234	45.831	0.00%	0.00%	-1.88%	-9.01%	0.00%	-0.40%	-1.88%	-9.37%	0.04%	7.47%	-1.84%	-9.00%
100	50%	0.01	5	45.418	31.324	0.00%	0.00%	-1.83%	-6.84%	0.00%	-0.03%	-1.83%	-6.85%	0.05%	45.06%	-1.78%	-6.82%
100	50%	0.0625	5	46.459	36.241	0.00%	0.00%	-1.77%	-5.98%	0.00%	-0.05%	-1.77%	-6.02%	0.05%	28.25%	-1.73%	-5.97%
120	50%	0.01	1	49.018	44.594	0.00%	0.00%	-1.89%	-9.30%	0.00%	-0.64%	-1.90%	-10.69%	0.03%	9.95%	-1.86%	-9.30%
120	50%	0.0625	1	49.234	45.831	0.00%	0.00%	-1.88%	-9.01%	0.00%	-0.70%	-1.89%	-10.56%	0.03%	7.46%	-1.85%	-9.01%
120	50%	0.01	5	45.418	31.324	0.00%	0.00%	-1.83%	-6.84%	0.00%	-0.08%	-1.83%	-7.03%	0.03%	45.04%	-1.79%	-6.83%
120	50%	0.0625	5	46.459	36.241	0.00%	0.00%	-1.77%	-5.98%	0.00%	-0.20%	-1.78%	-6.47%	0.03%	28.23%	-1.74%	-5.97%

Table 3: Comparison of VSR Methodologies - Heston Model

Note: The relative error between the model variance swap rate for a standard (geometric) variance swap and GVSR, and the error relative to its approximation AVSR*. Results are shown at two maturities, $T = 30$ and $T = 180$ and with 3 sets of strike price ranges. The first set of error results (labelled $k = [5 : 0.1 : 500]$) includes strikes starting at 5, ending at 500 with $dk = 0.1$ so that there is virtually no numerical error for GVSR. We do this so that the errors from using AVSR* can be isolated. The next four columns (11 – 13) isolate the effect of truncation error using set $k = [25 : 0.1 : 175]$ which includes strikes starting at 25, ending at 175 with $dk = 0.1$. The last set isolates the effect of discretisation error using set $k = [5 : 1 : 500]$ which includes strikes starting at 5, ending at 500 with $dk = 1$. All option prices are priced using the (Heston [1993]) model with $S_0 = [80, 100, 120]$, under low and high volatility regimes $V_0 = [20\%, 50\%]$. All other model parameter values are set as described in Section 5. The true GVSR is obtained using (4).

Entire Sample (12/10/92 - 22/12/15)									
Maturity	**30**	**60**	**90**	**120**	**150**	**180**	**210**	**240**	**270**
					GVSR				
Mean	20.02	20.08	20.13	20.44	20.81	20.89	20.84	20.76	20.69
StDev	8.395	7.833	7.256	7.044	6.981	6.789	6.593	6.433	6.288
Skewness	1.875	1.549	1.317	1.223	1.154	1.053	0.969	0.913	0.877
Kurtosis	5.145	3.159	1.959	1.651	1.413	1.004	0.659	0.431	0.315
					AVSR*				
Mean	19.27	19.18	19.09	19.14	19.30	19.25	19.11	18.97	18.85
StDev	7.969	7.245	6.646	6.361	6.237	6.030	5.829	5.669	5.531
Skewness	1.814	1.531	1.336	1.279	1.242	1.161	1.097	1.051	1.017
Kurtosis	4.869	3.181	2.156	1.967	1.848	1.512	1.228	1.036	0.933
Banking Crisis (01/09/08 - 31/03/09)									
Maturity	**30**	**60**	**90**	**120**	**150**	**180**	**210**	**240**	**270**
					GVSR				
Mean	45.31	42.72	39.72	39.17	39.93	39.19	38.16	37.37	36.9
StDev	11.82	9.655	8.023	8.09	7.671	6.918	6.326	5.933	5.668
Skewness	0.581	0.134	-0.006	-0.073	-0.411	-0.593	-0.736	-0.885	-1.038
Kurtosis	0.254	-0.392	-0.656	-0.552	-0.388	-0.169	-0.032	0.105	0.233
					AVSR*				
Mean	43.31	40.36	37.59	36.66	37.01	36.29	35.35	34.60	34.09
StDev	10.950	8.818	7.389	7.335	6.988	6.357	5.857	5.544	5.309
Skewness	0.603	0.191	0.010	-0.051	-0.338	-0.512	-0.653	-0.766	-0.880
Kurtosis	0.384	-0.144	-0.414	-0.435	-0.320	-0.127	-0.012	0.076	0.163

Table 4: VFTSE Descriptive Statistics
First four moments of the VSTE term structure distribution over the historical sample, 12 October 1992 to 22 December 2015. The lower part of the table shows the moments during the banking crisis period, September 2008 to March 2009. Two sets of moments are calculated in each case, the moments of the GVSR (4) and those of the AVSR*, (**??**).

Entire Sample (12/10/92 - 22/12/15)									
Maturity	**30**	**60**	**90**	**120**	**150**	**180**	**210**	**240**	**270**
					ASSR				
Mean	-1.06	-0.98	-0.89	-0.89	-0.90	-0.87	-0.82	-0.77	-0.72
StDev	0.485	0.446	0.419	0.396	0.400	0.404	0.398	0.387	0.382
Skewness	-1.104	-0.274	0.098	0.224	0.323	0.425	0.527	0.625	0.612
Kurtosis	2.670	0.599	-0.053	-0.128	-0.160	-0.102	0.027	0.236	0.280
					AKSR				
Mean	3.22	2.24	1.55	1.40	1.48	1.24	0.94	0.67	0.44
StDev	3.133	2.222	1.768	1.643	1.614	1.533	1.407	1.286	1.203
Skewness	2.779	1.952	1.181	1.000	0.749	0.606	0.493	0.404	0.418
Kurtosis	12.030	8.267	2.382	1.637	0.242	-0.226	-0.501	-0.641	-0.493
Banking Crisis (01/09/08 - 31/03/09)									
Maturity	**30**	**60**	**90**	**120**	**150**	**180**	**210**	**240**	**270**
					ASSR				
Mean	-0.60	-0.47	-0.32	-0.30	-0.28	-0.22	-0.15	-0.09	-0.05
StDev	0.184	0.230	0.271	0.237	0.177	0.175	0.173	0.171	0.177
Skewness	0.169	0.172	0.247	0.122	0.077	0.168	0.113	0.149	0.278
Kurtosis	-0.201	-0.240	-0.002	0.133	0.032	-0.039	0.018	-0.037	-0.138
					AKSR				
Mean	0.46	-0.23	-0.71	-0.83	-0.59	-0.62	-0.70	-0.74	-0.75
StDev	0.580	0.493	0.653	0.647	0.333	0.276	0.244	0.201	0.169
Skewness	0.096	0.574	0.335	0.230	0.986	0.702	0.720	0.734	0.600
Kurtosis	-0.447	0.301	-1.105	-0.502	1.176	0.316	0.237	0.502	0.472

Table 5: ASSR and AKSR Descriptive Statistics, FTSE 100
First four moments of the ASSR and AKSR term structure distribution over the historical sample, 12 October 1992 to 22 December 2015. The lower part of the table shows the moments during the banking crisis period, September 2008 to March 2009. Two sets of moments are calculated in each case, the moments of the ASSR (14) and those of the AKSR, (15).

Figure 10: Correlations between Arithmetic Moment Swap Rates
Correlations betweeen the AVSR, A3SR and A4SR over the entire historical sample (12 October 1992 and 22 December 2015) on the left, and during the banking crisis period (1 September 2008 and 31 March 2009) on the right.